



CMS-TOP-20-008

CERN-EP-2022-245
2023/11/30

Measurement of the top quark mass using a profile likelihood approach with the lepton+jets final states in proton-proton collisions at $\sqrt{s} = 13$ TeV

The CMS Collaboration^{*}

Abstract

The mass of the top quark is measured in 36.3 fb^{-1} of LHC proton-proton collision data collected with the CMS detector at $\sqrt{s} = 13$ TeV. The measurement uses a sample of top quark pair candidate events containing one isolated electron or muon and at least four jets in the final state. For each event, the mass is reconstructed from a kinematic fit of the decay products to a top quark pair hypothesis. A profile likelihood method is applied using up to four observables per event to extract the top quark mass. The top quark mass is measured to be $171.77 \pm 0.37\text{ GeV}$. This approach significantly improves the precision over previous measurements.

We dedicate this paper to the memory of our friend and colleague Thomas Ferbel, whose innovative work on precision measurements of the top quark mass laid the foundation for this publication.

Published in the European Physical Journal C as doi:10.1140/epjc/s10052-023-12050-4.

1 Introduction

The top quark [1, 2] is the most massive fundamental particle and its mass, m_t , is an important free parameter of the standard model (SM) of particle physics. Because of its large Yukawa coupling, the top quark dominates the higher-order corrections to the Higgs boson mass and a precise determination of m_t sets strong constraints on the stability of the electroweak vacuum [3, 4]. In addition, precise measurements of m_t can be used to test the internal consistency of the SM [5–7].

At the CERN LHC, top quarks are produced predominantly in quark-antiquark pairs ($t\bar{t}$), which decay almost exclusively into a bottom (b) quark and a W boson. Each $t\bar{t}$ event can be classified by the subsequent decay of the W bosons. For this paper, the lepton+jets channel is analyzed, where one W boson decays hadronically, and the other leptonically. Hence, the minimal final state consists of a muon or electron, at least four jets, and one undetected neutrino. This includes events where a muon or electron from a tau lepton decay passes the selection criteria.

The mass of the top quark has been measured with increasing precision using the reconstructed invariant mass of different combinations of its decay products [8]. The measurements by the Tevatron collaborations led to a combined value of $m_t = 174.30 \pm 0.65$ GeV [9], while the ATLAS and CMS Collaborations measured $m_t = 172.69 \pm 0.48$ GeV [10] and $m_t = 172.44 \pm 0.48$ GeV [11], respectively, from the combination of their most precise results at $\sqrt{s} = 7$ and 8 TeV (Run 1). The LHC measurements achieved a relative precision on m_t of 0.28%. These analyses extract m_t by comparing data directly to Monte Carlo simulations for different values of m_t . An overview of the discussion of this mass definition and its relationship to a theoretically well-defined parameter is presented in Ref. [12].

In the lepton+jets channel, m_t was measured by the CMS Collaboration with proton-proton (pp) collision data at $\sqrt{s} = 13$ TeV. The result of $m_t = 172.25 \pm 0.63$ GeV [13] was extracted using the ideogram method [14, 15], which had previously been employed in Run 1 [11]. In contrast to the Run 1 analysis, in the analysis of $\sqrt{s} = 13$ TeV data, the renormalization and factorization scales in the matrix-element (ME) calculation and the scales in the initial- and final-state parton showers (PS) were varied separately, in order to evaluate the corresponding systematic uncertainties. In addition, the impacts of extended models of color reconnection (CR) were evaluated. These models were not available for the Run 1 measurements and their inclusion resulted in an increase in the systematic uncertainty [13].

In this paper, we use a new mass extraction method on the same data, corresponding to 36.3 fb^{-1} , that were used in Ref. [13]. In addition to developments in the mass extraction technique, the reconstruction and calibration of the analyzed data have been improved, and updated simulations are used. For example, the underlying event tune CP5 [16] and the jet flavor tagger DEEPJET [17] were not available in the former analysis on the data. The new analysis employs a kinematic fit of the decay products to a $t\bar{t}$ hypothesis. For each event, the best matching assignment of the jets to the decay products is used. A profile likelihood fit is performed using up to four different observables for events that are well reconstructed by the kinematic fit and one observable for the remaining events. The additional observables are used to constrain the main sources of systematic uncertainty. The model for the likelihood incorporates the effects of variations of these sources, represented by nuisance parameters based on simulation, as well as the finite size of the simulated samples. This reduces the influence of systematic uncertainties in the measurement. Tabulated results are provided in the HEPData record for this analysis [18].

2 The CMS detector and event reconstruction

The central feature of the CMS apparatus is a superconducting solenoid of 6 m internal diameter, which provides a magnetic field of 3.8 T. Within the solenoid volume are a silicon pixel and strip tracker, a lead tungstate crystal electromagnetic calorimeter (ECAL), and a brass and scintillator hadron calorimeter (HCAL), each composed of a barrel and two endcap sections. Forward calorimeters extend the pseudorapidity (η) coverage provided by the barrel and endcap detectors. Muons are measured in gas-ionization detectors embedded in the steel flux-return yoke outside the solenoid. A more detailed description of the CMS detector, together with a definition of the coordinate system used and the relevant kinematic variables, can be found in Ref. [19].

The primary vertex is taken to be the vertex corresponding to the hardest scattering in the event, evaluated using tracking information alone, as described in Section 9.4.1 of Ref. [20]. The particle-flow (PF) algorithm [21] aims to reconstruct and identify each individual particle in an event, with an optimized combination of information from the various elements of the CMS detector. The energy of photons is obtained from the ECAL measurement. The energy of electrons is determined from a combination of the electron momentum at the primary interaction vertex as determined by the tracker, the energy of the corresponding ECAL cluster, and the energy sum of all bremsstrahlung photons spatially compatible with originating from the electron track. The energy of muons is obtained from the curvature of the corresponding track. The energy of charged hadrons is determined from a combination of their momentum measured in the tracker and the matching ECAL and HCAL energy deposits, corrected for the response function of the calorimeters to hadronic showers. Finally, the energy of neutral hadrons is obtained from the corresponding corrected ECAL and HCAL energy deposits.

Jets are clustered from PF candidates using the anti- k_T algorithm with a distance parameter of 0.4 [22, 23]. The jet momentum is determined as the vectorial sum of all particle momenta in the jet, and is found from simulation to be, on average, within 5 to 10% of the true momentum over the whole transverse momentum (p_T) spectrum and detector acceptance. Additional pp interactions within the same or nearby bunch crossings (pileup) can contribute additional tracks and calorimetric energy depositions, increasing the apparent jet momentum. To mitigate this effect, tracks identified as originating from pileup vertices are discarded and an offset correction is applied to correct for remaining contributions. Jet energy corrections are derived from simulation studies so that the average measured energy of jets becomes identical to that of particle level jets. In situ measurements of the momentum balance in dijet, photon+jet, Z+jet, and multijet events are used to determine any residual differences between the jet energy scale in data and in simulation, and appropriate corrections are made [24]. Additional selection criteria are applied to each jet to remove jets potentially dominated by instrumental effects or reconstruction failures. The jet energy resolution amounts typically to 15–20% at 30 GeV, 10% at 100 GeV, and 5% at 1 TeV [24]. Jets originating from b quarks are identified using the DEEP-JET algorithm [17, 25, 26]. This has an efficiency of approximately 78%, at a misidentification probability of 1% for light-quark and gluon jets and 12% for charm-quark jets [17, 26].

The missing transverse momentum vector, \vec{p}_T^{miss} , is computed as the negative vector sum of the transverse momenta of all the PF candidates in an event, and its magnitude is denoted as p_T^{miss} [27]. The \vec{p}_T^{miss} is modified to account for corrections to the energy scale of the reconstructed jets in the event.

The momentum resolution for electrons with $p_T \approx 45$ GeV from $Z \rightarrow ee$ decays ranges from 1.6 to 5.0%. It is generally better in the barrel region than in the endcaps, and also depends on the bremsstrahlung energy emitted by the electron as it traverses the material in front of the

ECAL [28, 29].

Muons are measured in the pseudorapidity range $|\eta| < 2.4$, with detection planes made using three technologies: drift tubes, cathode strip chambers, and resistive plate chambers. Matching muons to tracks measured in the silicon tracker results in a relative transverse momentum resolution, for muons with p_T up to 100 GeV, of 1% in the barrel and 3% in the endcaps. The p_T resolution in the barrel is better than 7% for muons with p_T up to 1 TeV [30].

3 Data samples and event selection

The analyzed data sample has been collected with the CMS detector in 2016 at a center-of-mass energy $\sqrt{s} = 13$ TeV. It corresponds to an integrated luminosity of 36.3 fb^{-1} [31]. Events are required to pass a single-electron trigger with a p_T threshold for isolated electrons of 27 GeV or a single-muon trigger with a minimum threshold on the p_T of an isolated muon of 24 GeV [32].

Simulated $t\bar{t}$ signal events are generated with the POWHEG v2 ME generator [33–35], PYTHIA8.219 PS [36], and use the CP5 underlying event tune [16] with top quark mass values, m_t^{gen} , of 169.5, 172.5, and 175.5 GeV. To model parton distribution functions (PDFs), the NNPDF3.1 next-to-next-to-leading order (NNLO) set [37, 38] is used with the strong coupling constant set to $\alpha_S = 0.118$. The various background samples are simulated with the same ME generators and matching techniques [39–43] as in Ref. [13]. The background processes are W/Z+jets, single-top, diboson, and events composed uniquely of jets produced through the strong interaction, referred to as quantum chromodynamics (QCD) multijet events. The PS simulation and hadronization is performed with PYTHIA8, using the CUETP8M1 tune [44].

All of the simulated samples are processed through a full simulation of the CMS detector based on GEANT4 [45] and are normalized to their predicted cross section described in Refs. [46–49]. The effects of pileup are included in the simulation and the pileup distribution in simulation is weighted to match the pileup in the data. The jet energy response and resolution in simulated events are corrected to match the data [24]. In addition, the b-jet identification (b tagging) efficiency and misidentification rate [25], and the lepton trigger and reconstruction efficiencies are corrected in simulation [28, 30].

Events are selected with exactly one isolated electron (muon) with $p_T > 29$ (26) GeV and $|\eta| < 2.4$ that is separated from PF jet candidates with $\Delta R = \sqrt{(\Delta\eta)^2 + (\Delta\phi)^2} > 0.3$ (0.4), where $\Delta\eta$ and $\Delta\phi$ are the differences in pseudorapidity and azimuth (in radians) between the jet and lepton candidate. The four leading jet candidates in each event are required to have $p_T > 30$ GeV and $|\eta| < 2.4$. Only these four jets are used in further reconstruction. Exactly two b-tagged jets are required among the four selected jets, yielding 287 842 (451 618) candidate events in the electron+jets (muon+jets) decay channel.

To check the compatibility of an event with the $t\bar{t}$ hypothesis, and to improve the resolution of the reconstructed quantities, a kinematic fit [50] is performed. For each event, the inputs to the algorithm are the momenta of the lepton and of the four leading jets, \vec{p}_T^{miss} , and the resolutions of these variables. The fit constrains these quantities to the hypothesis that two heavy particles of equal mass are produced, each one decaying to a b quark and a W boson, with the invariant mass of the latter constrained to 80.4 GeV. The kinematic fit then minimizes $\chi^2 \equiv (\mathbf{x} - \mathbf{x}^m)^T G(\mathbf{x} - \mathbf{x}^m)$ where \mathbf{x}^m and \mathbf{x} are the vectors of the measured and fitted momenta, respectively, and G is the inverse covariance matrix, which is constructed from the uncertainties in the measured momenta. The masses are fixed to 5 GeV for the b quarks and to zero for the light quarks and leptons. The two b-tagged jets are candidates for the b quarks in the $t\bar{t}$

hypothesis, while the two jets that are not b tagged serve as candidates for the light quarks from the hadronically decaying W boson. This leads to two possible parton-jet assignments, each with two solutions for the longitudinal component of the neutrino momentum, and four different permutations per event. For simulated $t\bar{t}$ events, the parton-jet assignments can be classified as correct permutations, wrong permutations, and unmatched permutations, where, in the latter case, at least one quark from the $t\bar{t}$ decay is not unambiguously matched within a distance of $\Delta R < 0.4$ to any of the four selected jets.

The goodness-of-fit probability, $P_{\text{gof}} = \exp(-\chi^2/2)$, is used to determine the most likely parton-jet assignment. For each event, the observables from the permutation with the highest P_{gof} value are the input to the m_t measurement. In addition, the events are categorized as either $P_{\text{gof}} < 0.2$ or $P_{\text{gof}} > 0.2$, matching the value chosen in Ref. [13]. Requiring $P_{\text{gof}} > 0.2$ yields 87 265 (140 362) $t\bar{t}$ candidate events in the electron+jets (muon+jets) decay channel and has a predicted signal fraction of 95%. This selection improves the fraction of correctly reconstructed events from 20 to 47%. Figure 1 shows the distribution of the invariant mass of the hadronically decaying top quark candidate before (m_t^{reco}) and after (m_t^{fit}) the $P_{\text{gof}} > 0.2$ selection and the kinematic fit. A large part of the depicted uncertainties on the expected event yields are correlated. Hence, the overall normalization of the simulation agrees within the uncertainties, although the simulation predicts 10% more events in all distributions. For the final measurement, the simulation is normalized to the number of events observed in data.

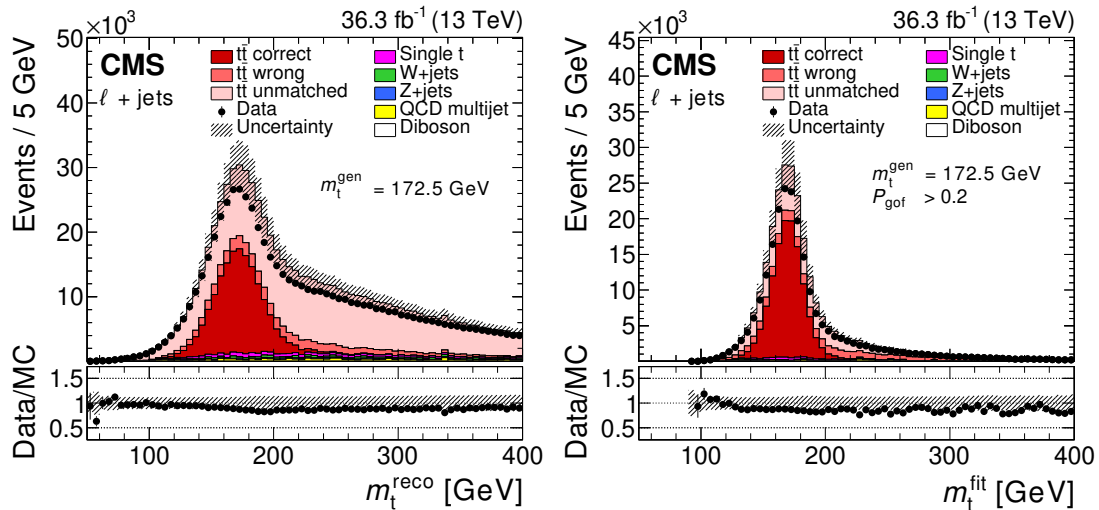


Figure 1: The top quark mass distribution before (left) and after (right) the $P_{\text{gof}} > 0.2$ selection and the kinematic fit. For the simulated $t\bar{t}$ events, the jet-parton assignments are classified as correct, wrong, and unmatched permutations, as described in the text. The uncertainty bands contain statistical uncertainties in the simulation, normalization uncertainties due to luminosity and cross section, jet energy correction uncertainties, and all uncertainties that are evaluated from event-based weights. A large part of the depicted uncertainties on the expected event yields are correlated. The lower panels show the ratio of data to the prediction. A value of $m_t^{\text{gen}} = 172.5 \text{ GeV}$ is used in the simulation.

4 Observables and systematic uncertainties

Different observables are used per event based on its P_{gof} value. The cases and observables are listed in Table 1.

Table 1: The overall list of different input histograms and their inclusion in a certain histogram set. A histogram marked with “ \times ” is included in a set (measurement).

Observable	Histogram Category	Set label				
		1D	2D	3D	4D	5D
m_t^{fit}	$P_{\text{gof}} > 0.2$	\times	\times	\times	\times	\times
m_W^{reco}	$P_{\text{gof}} > 0.2$		\times	\times	\times	\times
$m_{\ell b}^{\text{reco}}$	$P_{\text{gof}} < 0.2$			\times	\times	\times
$m_{\ell b}^{\text{reco}} / m_t^{\text{fit}}$	$P_{\text{gof}} > 0.2$				\times	\times
$R_{\text{bq}}^{\text{reco}}$	$P_{\text{gof}} > 0.2$					\times

For events with $P_{\text{gof}} > 0.2$, the mass of the top quark candidates from the kinematic fit, m_t^{fit} , shows a very strong dependence on m_t and is the main observable in this analysis. Only events with m_t^{fit} values between 130 and 350 GeV are used in the measurement. The high mass region is included to constrain the contribution of unmatched events to the peak. For events with $P_{\text{gof}} < 0.2$, the invariant mass of the lepton and the b-tagged jet assigned to the semileptonically decaying top quark, $m_{\ell b}^{\text{reco}}$, is shown in Fig. 2 (right). For most $t\bar{t}$ events, a low P_{gof} value is caused by assigning a wrong jet to the W boson candidate, while the correct b-tagged jets are the candidates for the b quarks in 60% of these events. Hence, $m_{\ell b}^{\text{reco}}$ preserves a good m_t dependence and adds additional sensitivity to the measurement. The measurement is limited to $m_{\ell b}^{\text{reco}}$ values between 0 and 300 GeV. While a similar observable has routinely been used in m_t measurements in the dilepton channel [51, 52], this is the first application of this observable in the lepton+jets channel.

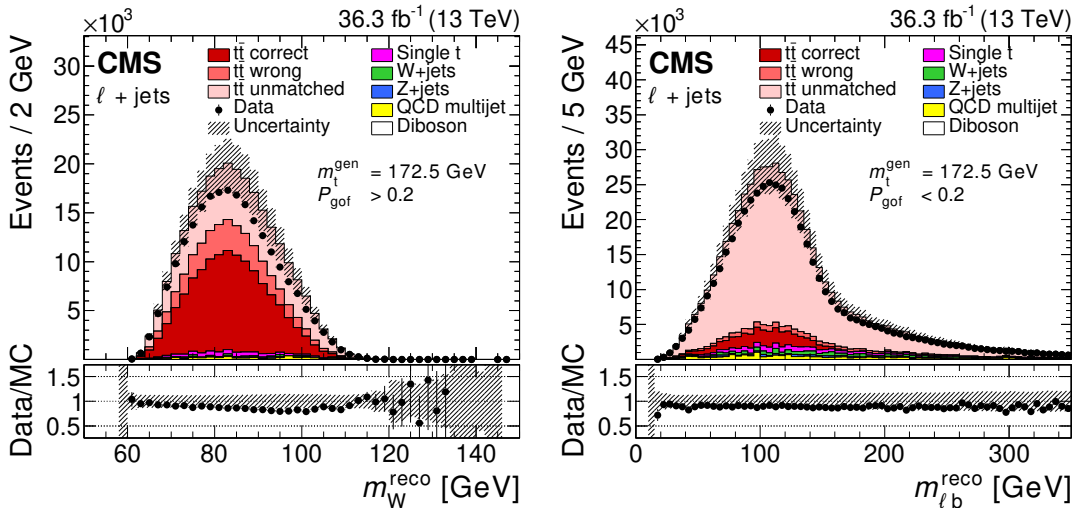


Figure 2: The distributions of the reconstructed W boson mass for the $P_{\text{gof}} > 0.2$ category (left) and of the invariant mass of the lepton and the jet assigned to the semileptonic decaying top quark for the $P_{\text{gof}} < 0.2$ category (right). The uncertainty bands contain statistical uncertainties in the simulation, normalization uncertainties due to luminosity and cross section, jet energy correction uncertainties, and all uncertainties that are evaluated from event-based weights. A large part of the depicted uncertainties on the expected event yields are correlated. The lower panels show the ratio of data to the prediction. A value of $m_t^{\text{gen}} = 172.5$ GeV is used in the simulation.

Additional observables are used in parallel for the mass extraction to constrain systematic uncertainties. In previous analyses by the CMS Collaboration in the lepton+jets channel [11, 13],

the invariant mass of the two untagged jets before the kinematic fit, m_W^{reco} , has been used together with m_t^{fit} , mainly to reduce the uncertainty in the jet energy scale and the jet modeling. Its distribution is shown in Fig. 2 (left) and the region between 63 and 110 GeV is used in the measurement. As m_W^{reco} is only sensitive to the energy scale and modeling of light flavor jets, two additional observables are employed to improve sensitivity to the scale and modeling of jets originating from b quarks. These are the ratio $m_{\ell b}^{\text{reco}} / m_t^{\text{fit}}$, and the ratio of the scalar sum of the transverse momenta of the two b-tagged jets (b1, b2), and the two non-b-tagged jets (q1, q2), $R_{\text{bq}}^{\text{reco}} = (p_T^{\text{b1}} + p_T^{\text{b2}}) / (p_T^{\text{q1}} + p_T^{\text{q2}})$. Their distributions are shown in Fig. 3. While m_t^{fit} and m_W^{reco} have been used by the CMS Collaboration in previous analyses in the lepton+jets channel, $m_{\ell b}^{\text{reco}}$, $m_{\ell b}^{\text{reco}} / m_t^{\text{fit}}$, and $R_{\text{bq}}^{\text{reco}}$ are new additions. However, $R_{\text{bq}}^{\text{reco}}$ has been used in the lepton+jets channel by the ATLAS Collaboration [10, 53].

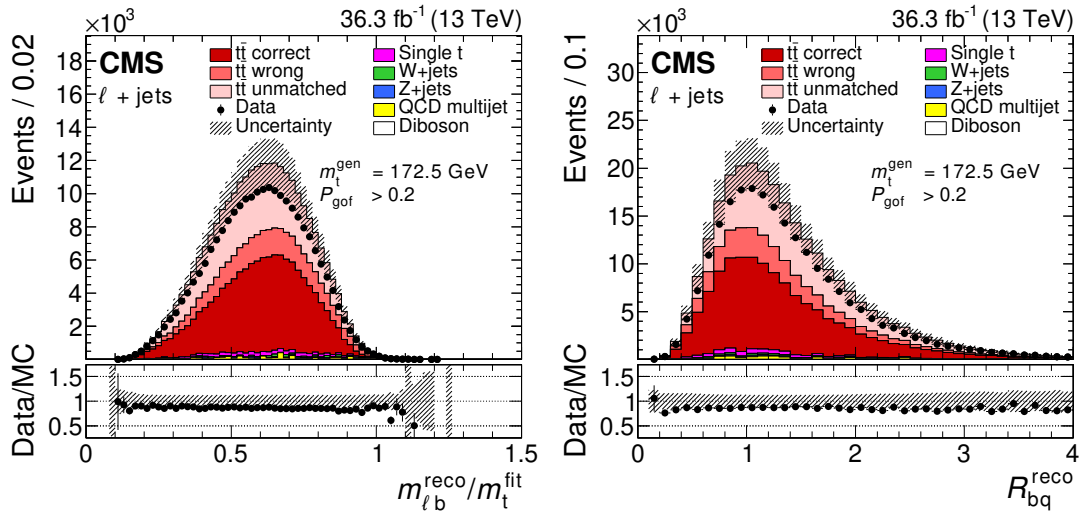


Figure 3: The distributions of $m_{\ell b}^{\text{reco}} / m_t^{\text{fit}}$ (left) and of $R_{\text{bq}}^{\text{reco}}$ (right), both for the $P_{\text{gof}} > 0.2$ category. The uncertainty bands contain statistical uncertainties in the simulation, normalization uncertainties due to luminosity and cross section, jet energy correction uncertainties, and all uncertainties that are evaluated from event-based weights. A large part of the depicted uncertainties on the expected event yields are correlated. The lower panels show the ratio of data to the prediction. A value of $m_t^{\text{gen}} = 172.5 \text{ GeV}$ is used in the simulation.

The distributions of the five observables are affected by uncertainties in the modeling and the reconstruction of the simulated events. These sources of systematic uncertainties are nearly identical to those in the previous measurements [13, 54]. The only difference is that we no longer include a systematic uncertainty related to the choice of ME generator as this uncertainty would overlap with the uncertainty we find from varying the default ME generator parameters. The considered sources are summarized in the categories listed below.

- *Method calibration:* In the previous measurements [13, 54], the limited size of the simulated samples for different values of m_t^{gen} lead to an uncertainty in the calibration of the mass extraction method. In the new profile likelihood approach, the statistical uncertainty in the top quark mass dependence due to the limited sample size is included via nuisance parameters.
- *Jet energy correction (JEC):* Jet energies are scaled up and down according to the p_T - and η -dependent data/simulation uncertainties [24, 55]. Each of the 25 individual uncertainties in the jet energy corrections is represented by its own nuisance parameter.

- *Jet energy resolution* (JER): Since the JER measured in data is worse than in simulation, the simulation is modified to correct for the difference [24, 55]. The jet energy resolution in the simulation is varied up and down within the uncertainty. The variation is evaluated independently for two $|\eta_{\text{jet}}|$ regions, split at $|\eta_{\text{jet}}| = 1.93$.
- *b tagging*: The p_T -dependent uncertainty of the b-tagging efficiencies and misidentification rates of the DEEPJET tagger [17, 26] are taken into account by reweighting the simulated events accordingly.
- *Pileup*: To estimate the uncertainty from the determination of the number of pileup events and the reweighting procedure, the inelastic pp cross section [56] used in the determination is varied by $\pm 4.6\%$.
- *Background* (BG): The main uncertainty in the background stems from the uncertainty in the measurements of the cross sections used in the normalization. The normalization of the background samples is varied by $\pm 10\%$ for the single top quark samples [57, 58], $\pm 30\%$ for the W+jets samples [59], $\pm 10\%$ for the Z+jets [60] and for the diboson samples [61, 62], and $\pm 100\%$ for the QCD multijet samples. The size of the variations is the same as in the previous measurement [13] in this channel. The uncertainty in the luminosity of 1.2% [31] is negligible compared to these variations.
- *Lepton scale factors* (SFs) *and momentum scale*: The simulation-to-data scale factors for the trigger, reconstruction, and selection efficiencies for electrons and muons are varied within their uncertainties. In addition, the lepton energy in simulation is varied up and down within its uncertainty.
- *JEC flavor*: The difference between Lund string fragmentation and cluster fragmentation is evaluated by comparing PYTHIA 6.422 [63] and HERWIG++ 2.4 [64]. The jet energy response is compared separately for each jet flavor [24].
- *b-jet modeling* (bJES): The uncertainty associated with the fragmentation of b quarks is split into four components. The Bowler–Lund fragmentation function is varied symmetrically within its uncertainties, as determined by the ALEPH and DELPHI Collaborations [65, 66]. The difference between the default PYTHIA setting and the center of the variations is included as an additional uncertainty. As an alternative model of the fragmentation into b hadrons, the Peterson fragmentation function is used and the difference obtained relative to the Bowler–Lund fragmentation function is assigned as an uncertainty. The third uncertainty source taken into account is the semileptonic b-hadron branching fraction, which is varied by -0.45 and $+0.77\%$, motivated by measurements of B^0/B^+ decays and their corresponding uncertainties [8] and a comparison of the measured branching ratios to PYTHIA.
- *PDF*: The default PDF set in the simulation, NNPDF3.1 NNLO [37, 38], is replaced with the CT14 NNLO [67] and MMHT 2014 NNLO [68] PDFs via event weights. In addition, the default set is varied with 100 Hessian eigenvectors [38] and the α_S value is changed to 0.117 and 0.119. All described variations are evaluated for their impact on the measurement and the negligible variations are later omitted to reduce the number of nuisance parameters.
- *Renormalization and factorization scales*: The renormalization and factorization scales for the ME calculation are varied independently and simultaneously by factors of 2 and 1/2. This is achieved by reweighting the simulated events. The independent variations were checked and it was found to be sufficient to include only the simultaneous variations as a nuisance parameter.
- *ME to PS matching*: The matching of the POWHEG ME calculations to the PYTHIA PS

is varied by shifting the parameter $h_{\text{damp}} = 1.58^{+0.66}_{-0.59}$ [69] within its uncertainty.

- *ISR and FSR*: For initial-state radiation (ISR) and final-state radiation (FSR), 32 decorrelated variations of the renormalization scale and nonsingular terms for each branching type ($g \rightarrow gg$, $g \rightarrow q\bar{q}$, $q \rightarrow qg$, and $X \rightarrow Xg$ with $X = t$ or b) are applied using event weights [70]. The scale variations correspond to a change of the respective PS scale in PYTHIA by factors of 2 and 1/2. This approach is new compared to the previous analysis [13], which only evaluated correlated changes in the FSR and ISR PS scales.
- *Top quark p_T* : Recent calculations suggest that the top quark p_T spectrum is strongly affected by NNLO effects [71–73]. The p_T of the top quark in simulation is varied to match the distribution measured by CMS [74, 75]. The default simulation is not corrected for this effect, but this variation is included via a nuisance parameter in the m_t measurement.
- *Underlying event*: Measurements of the underlying event have been used to tune PYTHIA parameters describing nonperturbative QCD effects [16, 44]. The parameters of the tune are varied within their uncertainties.
- *Early resonance decays*: Modeling of color reconnection introduces systematic uncertainties, which are estimated by comparing different CR models and settings. In the default sample, the top quark decay products are not included in the CR process. This setting is compared to the case of including the decay products by enabling early resonance decays in PYTHIA8.
- *CR modeling*: In addition to the default model used in PYTHIA8, two alternative CR models are used, namely a model with string formation beyond leading color (“QCD inspired”) [76] and a model allowing the gluons to be moved to another string (“gluon move”) [77]. Underlying event measurements are used to tune the parameters of all models [78]. For each model, an individual nuisance parameter is introduced.

5 Mass extraction method

A maximum likelihood (ML) fit to the selected events is employed to measure m_t . The evaluated likelihood ratio $\lambda(m_t, \vec{\theta}, \vec{\beta}, \Omega | \text{data})$ depends not only on m_t , but also on three sets of nuisance parameters. The nuisance parameters, $\vec{\theta}$, incorporate the uncertainty in systematic effects, while the statistical nuisance parameters, $\vec{\beta}$ and Ω , incorporate the statistical uncertainties in the simulation. The parameters $\vec{\beta}$ account for the limited sample size of the default simulation and the parameters Ω account for the limited size in the simulated samples for variations of m_t and of the uncertainty sources. All nuisance parameters are normalized such that a value of 0 represents the absence of the systematic effect and the values ± 1 correspond to a variation of the systematic effect by one standard deviation up or down. The ROOFIT [79] package is used to define and evaluate all the functions. The minimum of the negative log-likelihood $-2 \ln \lambda(m_t, \vec{\theta}, \vec{\beta}, \Omega | \text{data})$ is found with the MINUIT2 package [80].

The data are characterized by up to four observables per event, as mentioned in Section 4. The events are split into the electron+jets and the muon+jets channels. The input to the ML fit is a set of one-dimensional histograms of the observables, x_i , in the two P_{gof} categories. For each histogram, a suitable probability density function $P(x_i | m_t, \vec{\theta}, \vec{\beta}, \Omega)$ is derived from simulation.

The probability density function for the m_t^{fit} histograms is approximated by the sum of a Voigt

profile (the convolution of a Cauchy–Lorentz distribution and a Gaussian distribution) for the correctly reconstructed $t\bar{t}$ candidates and Chebyshev polynomials for the remaining events. For all other observables, a binned probability density function is used that returns the relative fraction of events per histogram bin. Here, eight bins are used for each observable and the width of the bins is chosen so that each bin has a similar number of selected events for the default simulation ($m_t^{\text{gen}} = 172.5 \text{ GeV}$). For the following, we denote the parameters of the probability density functions as $\vec{\alpha}$. All the functions $P_i(x_i|\vec{\alpha})$ are normalized to the number of events in the histogram for the observable x_i , so only shape information is used in the ML fit. Hence, the parameters $\vec{\alpha}$ are correlated even for the binned probability density function. The dependence of these parameters on m_t and $\vec{\theta}$ is assumed to be linear. The full expression is for a component α_k of $\vec{\alpha}$

$$\alpha_k = C_k \left(1 + d_k \left[\alpha_k^0 + \sigma_k^\alpha \beta_k + s_k^0 (m_t - 172.5 \text{ GeV}) + \sigma_k^0 \Omega_k^0 \right] \right) \prod_l \left(1 + d_k \left[s_k^l \theta_l + \sigma_k^l \Omega_k^l \right] \right),$$

with l indicating the nuisance parameter. For the nuisance parameters corresponding to the FSR PS scale variations, the linear term, $s_k^l \theta_l$, is replaced with a second-order polynomial. With these expressions for the parameters α_k , the probability density function, $P_i(x_i|\vec{\alpha})$, for an observable x_i becomes the function $P_i(x_i|m_t, \vec{\theta}, \vec{\beta}, \Omega)$ mentioned above.

The model parameter α_k^0 is determined by a fit to the default simulation, while the linear dependencies of α_k on m_t or a component θ_l of $\vec{\theta}$ are expressed with the model parameters s_k^0 and s_k^l , respectively. The parameter s_k^0 is determined from a simultaneous fit to simulated samples, where m_t^{gen} is varied by $\pm 3 \text{ GeV}$ from the default value. Along the same lines, the parameters s_k^l are obtained from fits to the simulation of the systematic effect corresponding to the nuisance parameter θ_l . The values of C_k and d_k are chosen ad hoc so that the results of the fits of α_k^0 , s_k^0 , and the s_k^l are all of the same order of magnitude and with a similar statistical uncertainty. This improves the numerical stability of the final ML fit.

The limited size of the simulated samples for different m_t^{gen} values gives rise to a calibration uncertainty in m_t . Hence, additional statistical nuisance parameters, β_k and Ω_k^0 , are introduced that account for the statistical uncertainty in the model parameters α_k^0 and s_k^0 , similar to the Barlow–Beeston approach [81, 82]. They are scaled by σ_k^α and σ_k^0 , which are the standard deviations of α_k^0 and s_k^0 obtained from the fits to the default simulation or the m_t^{gen} -varied samples, respectively. Hence, a statistical nuisance with value $\Omega_k^0 = \pm 1$ changes the corresponding α_k , i.e., the shape or the bin content of an observable, by the statistical uncertainty in the m_t dependence evaluated at a shift in m_t of 1 GeV. Similarly, the parameters s_k^l contain random fluctuations if they are determined from simulated samples that are statistically independent to the default simulation and of limited size. These fluctuations can lead to overconstraints on the corresponding nuisance parameter θ_l and, hence, an underestimation of the systematic uncertainty. The nuisance parameters Ω_k^l are added to counter these effects and are scaled by parameters σ_k^l , which are the standard deviations of the s_k^l parameters from the fits to the corresponding samples for the systematic effect. As in the m_t case, a value of $\Omega_k^l = \pm 1$ changes the corresponding α_k by the statistical uncertainty in the θ_l dependence evaluated at a shift in θ_l of 1. Unlike the systematic nuisance parameters θ_l , which affect all α_k collectively, for each α_k there are individual Ω_k^l parameters. While this drastically increases the number of fitted parameters in the ML fit to data, this also guarantees that the Ω_k^l parameters are hardly constrained by the fit to data and the uncertainty in m_t includes the statistical uncertainty in the impact of the systematic effect.

For a single histogram in a set, the products of Poisson probabilities for the prediction $\mu_{i,j} = n_{\text{tot},i} P_i(x_{i,j}|m_t, \vec{\theta}, \vec{\beta}, \Omega)$ and for an alternative model with an adjustable parameter per bin $\hat{\mu}_{i,j} = n_{i,j}$ are used to compute the likelihood ratio λ_i [8], where x_i is the observable, $n_{i,j}$ is the content of bin j with bin center $x_{i,j}$, and $n_{\text{tot},i}$ is the total number of entries. Then the combined likelihood ratio for a set with observables \vec{x} is

$$\lambda(m_t, \vec{\theta}, \vec{\beta}, \Omega | \text{data}) = \left(\prod_i \lambda_i(m_t, \vec{\theta}, \vec{\beta}, \Omega | x_i) \right) \left(\prod_l P(\theta_l) \right) P(\vec{\beta}) P(\Omega),$$

where $P(\theta_l)$, $P(\vec{\beta})$, and $P(\Omega)$ are the pre-fit probability density functions of the nuisance parameters θ_l , $\vec{\beta}$, and Ω . The product of the likelihood ratios can be used on the right-hand side of the equation, as all observables are independent in most phase space regions. The probability density functions of the nuisance parameters related to the sources of systematic uncertainties, $P(\theta_l)$, are standard normal distributions. All model parameters α_k^0 , s_k^0 , or s_k^l that are related to the same observable and nuisance parameter are obtained together by one fit to the corresponding simulation samples. To take the correlations between these parameters into account, the statistical nuisance parameters $\vec{\beta}$ or Ω that incorporate the statistical uncertainty in these parameters are constrained by centered multivariate normal distributions. The covariances of the distributions are set to the correlation matrices obtained by the fits of the corresponding parameters. The latter nuisance parameters and constraints are only included if the model parameters are determined from samples that are statistically independent of the default simulation, like, for example, for the alternative color reconnection models. If the model parameters are determined from samples obtained from varying the default simulation with event-based weights or scaling or smearing of the jet energies, the corresponding Ω parameters are fixed to zero and the constraint is removed from $\lambda(m_t, \vec{\theta}, \vec{\beta}, \Omega | \text{data})$.

The mass of the top quark is determined with the profile likelihood fit for different sets of data histograms. The sets and their labels are listed in Table 1.

The expected total uncertainty in m_t is evaluated for each set defined in Table 1 with pseudo-experiments using the default simulation. The results of the pseudo-experiments are shown in Fig. 4 (left). The improvements in the data reconstruction and calibration, event selection, simulation, and mass extraction method reduce the uncertainty in the 1D measurement from 1.09 to 0.63 GeV, when compared to the previous measurement [13]. The uncertainty in the 2D measurement improves from 0.63 to 0.50 GeV. The additional observables and the split into categories further reduce the expected uncertainty down to 0.37 GeV for the 5D set.

The statistical uncertainty is obtained from fits that only have m_t as a free parameter. From studies on simulation, it is expected to be 0.07, 0.06, and 0.04 GeV in the electron+jets, muon+jets, and the combined (lepton+jets) channels, respectively.

The applied statistical model is verified with additional pseudo-experiments. Here, the data for one pseudo-experiment are generated using probability density functions $P(x_i|m_t, \vec{\theta})$ that have the same functional form as the ones used in the ML fit, but their model parameters $\vec{\alpha}$ and all slopes, s_k^l are determined on statistically fluctuated simulations. For the generation of a pseudo-experiment, m_t is chosen from a uniform distribution with a mean of 172.5 GeV and the same standard deviation as is assumed for the calibration uncertainty. The values of the nuisance parameters $\vec{\theta}$ are drawn from standard normal distributions. The same ML fit that is applied to the collider data is then performed on the pseudo-data. The pseudo-experiments are generated for two cases, specifically, with and without the statistical nuisance parameters $\vec{\beta}$ and Ω in the ML fit. Figure 4 (right) shows the distribution of the differences between the measured and

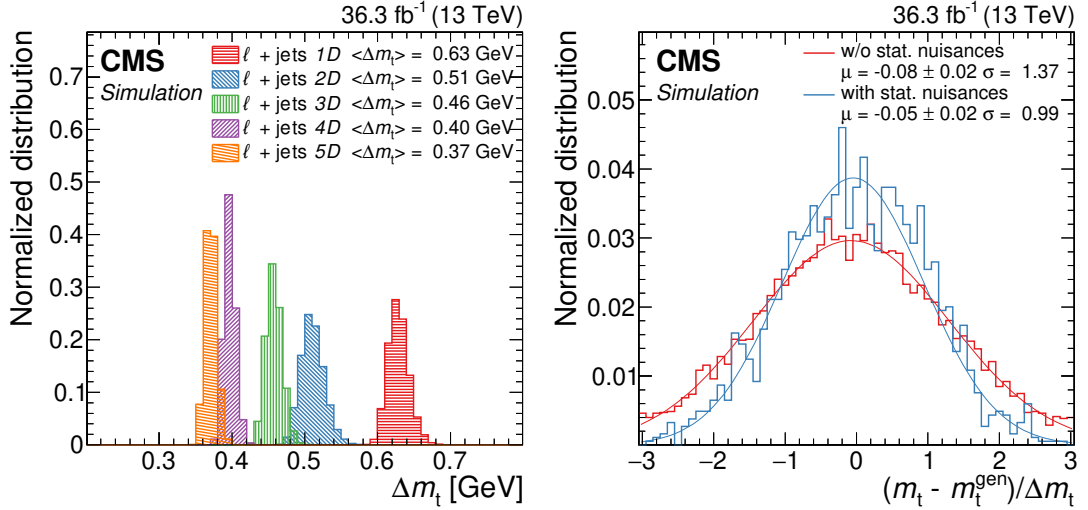


Figure 4: Left: Comparison of the expected total uncertainty in m_t in the combined lepton+jets channel and for the different observable-category sets defined in Table 1. Right: The difference between the measured and generated m_t values, divided by the uncertainty reported by the fit from pseudo-experiments without (red) or with (blue) the statistical nuisance parameters $\vec{\beta}$ and Ω in the 5D ML fit. Also included in the legend are the μ and σ parameters of Gaussian functions (red and blue lines) fit to the histograms.

generated m_t values, divided by the uncertainty reported by the fit for both cases. A nearly 40% underestimation of the measurement uncertainty can be seen for the case without the statistical nuisance parameters $\vec{\beta}$ and Ω , while consistency is observed for the method that is employed on data.

In addition, single-parameter fits were performed on pseudo-data sampled from simulation to verify that the mass extraction method is unbiased and reports the correct uncertainty. These tests were done for fits of m_t with samples corresponding to mass values of 169.5, 172.5, and 175.5 GeV, as well as on the simulation of different systematic effects for the fits of the corresponding nuisance parameter.

6 Results

The results of the profile likelihood fits to data are shown in Fig. 5 for the electron+jets, muon+jets, and lepton+jets channels and for the different sets of observables and categories, as defined in Table 1. The observables m_W^{reco} , $m_{\ell b}^{\text{reco}}/m_t^{\text{fit}}$, and $R_{\text{bq}}^{\text{reco}}$ provide constraints on the modeling of the $t\bar{t}$ decays in addition to the observables m_t^{fit} and $m_{\ell b}^{\text{reco}}|_{P_{\text{go}}<0.2}$, which are highly sensitive to m_t . With the profile likelihood method, these constraints not only reduce the uncertainty in m_t , but also change the measured m_t value, as they effectively alter the parameters of the reference $t\bar{t}$ simulation. When additional observables are included, the measurement in the lepton+jets channel yields a smaller mass value than the separate channels because of the correlations between the channels.

The 5D fit to the selected events results in the best precision and yields in the respective chan-

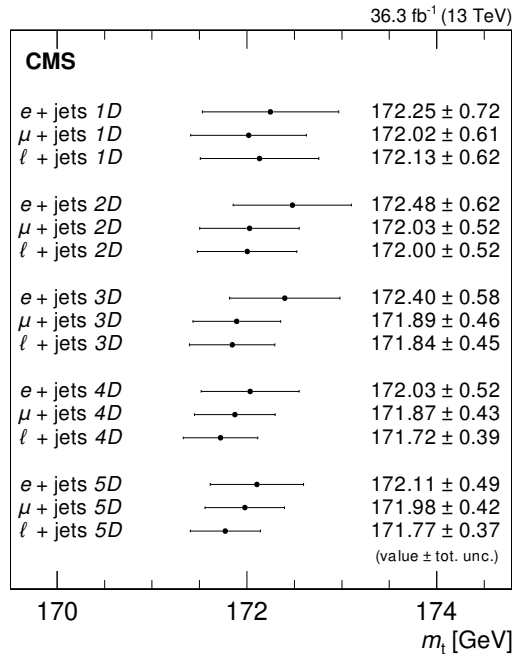


Figure 5: Measurement of m_t in the three different channels for the different sets of observables and categories as defined in Table 1.

nels:

$$\begin{aligned} \text{Electron+jets: } m_t^{5D} &= 172.11 \pm 0.49 \text{ GeV,} \\ \text{Muon+jets: } m_t^{5D} &= 171.98 \pm 0.42 \text{ GeV,} \\ \text{Lepton+jets: } m_t^{5D} &= 171.77 \pm 0.37 \text{ GeV.} \end{aligned}$$

The comparisons of the data distributions and the post-fit 5D model are shown in Fig. 6. While the binned probability density functions of the model describe the corresponding observables well, significant deviations between the data and the model can be observed in the peak region of the m_t^{fit} observable. These deviations are also observed in simulation and stem from the fact that effectively only two parameters, the peak position and its average width, are used in the model to describe the peak. Tests with simulation show no bias on the extracted m_t value from these deviations. In fact, the small number of parameters should increase the robustness of the measurement as the model is not sensitive to finer details of the peak shape that might be difficult to simulate correctly.

Figure 7 shows the pulls on the most important systematic nuisance parameters θ and their impacts on m_t , Δm_t , after the fit with the 5D model. The pulls are defined as $(\hat{\theta} - \theta_0)/\Delta\theta$, where $\hat{\theta}$ is the measured nuisance parameter value and θ_0 and $\Delta\theta$ are the mean and standard deviation of the nuisance parameter before the fit. The pre-fit impacts are evaluated by repeating the ML fit with the studied nuisance parameter θ fixed to $\hat{\theta} \pm \Delta\theta$ and taking the difference in m_t between the result of these fits and the measured m_t . In most cases, the post-fit impacts are evaluated respectively with $\hat{\theta}$ and $\widehat{\Delta\theta}$, where $\widehat{\Delta\theta}$ is the uncertainty in the nuisance parameter after the fit. However, if the studied systematic nuisance parameter θ has statistical nuisance parameters Ω that account for the statistical uncertainty in the θ -dependence of the model, the combined impact of the systematic and statistical nuisance parameters is plotted in Fig. 7 as post-fit impact. To estimate this combined impact, the likelihood fit is repeated with the corresponding systematic and statistical nuisance parameters fixed to their post-fit values and the quadratic

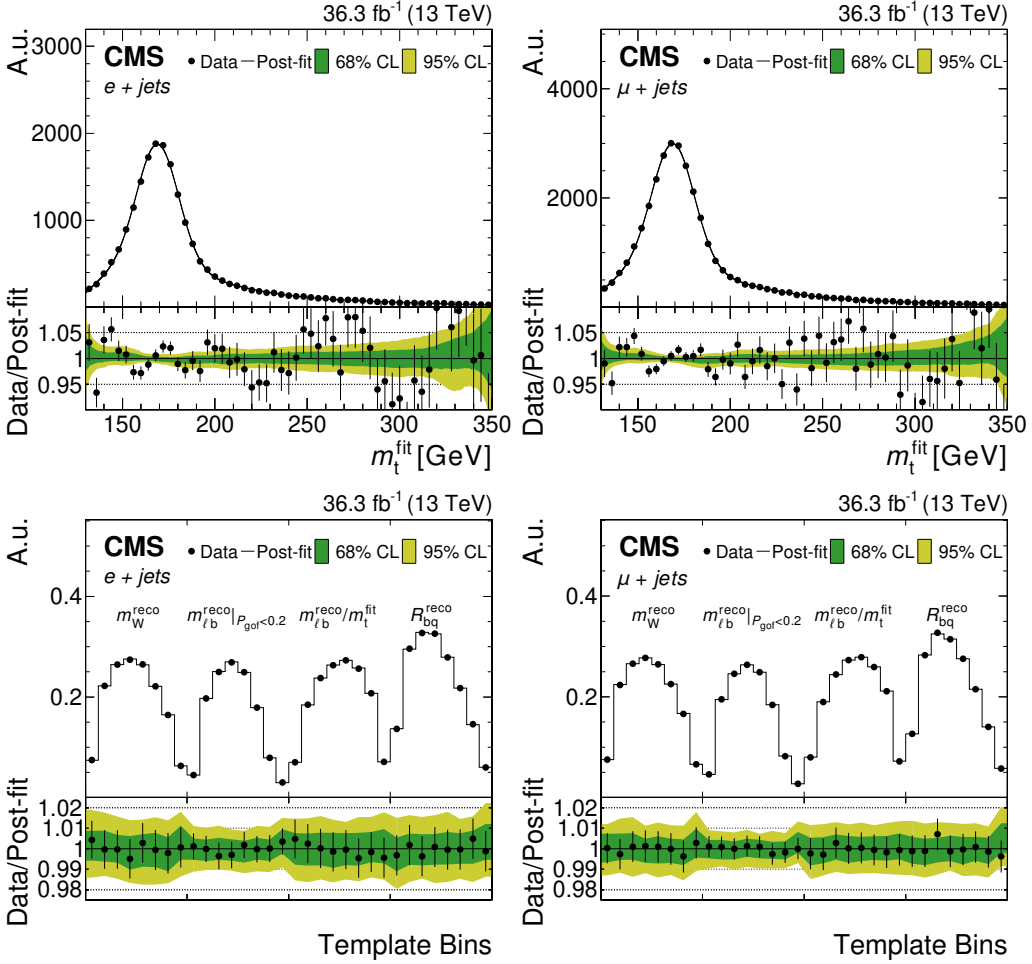


Figure 6: Distribution of m_t^{fit} (upper) and the additional observables (lower) that are the input to the 5D ML fit and their post-fit probability density functions for the combined fit to the electron+jets (left) and muon+jets (right) channels. For the additional observables results, the events in each bin are divided by the bin width. The lower panels show the ratio of data and post-fit template values. The green and yellow bands represent the 68 and 95% confidence levels in the fit uncertainty.

difference of the overall m_t uncertainty compared to the default fit is taken. The quadratic difference between the combined impact and the post-fit impact of only the systematic nuisance parameter is interpreted as the effect of the limited size of the systematic simulation samples.

Most nuisance parameters are consistent with their pre-fit values. The largest effect on the measured mass value corresponds to the FSR scale of the $q \rightarrow qg$ branching type. The effect is caused by the difference in the peak position of m_W^{reco} seen in Fig. 2 (left). The previous measurements in this channel by the CMS Collaboration assumed correlated FSR PS scales with the same scale choice for jets induced by light quarks and b quarks [11, 13]. In that case, a lower peak position in the m_W^{reco} distribution would also cause the m_t^{fit} peak position to be lower than expected from simulation for a given m_t value, resulting in a higher top quark mass value to be measured. In fact, a 5D fit to data assuming fully correlated FSR PS scale choices yields $m_t = 172.20 \pm 0.31$ GeV. This value is very close to the previous measurement on the same data of $m_t = 172.25 \pm 0.63$ GeV [13].

The measurement is repeated for different correlation coefficients (ρ_{FSR}) in the pre-fit covariance

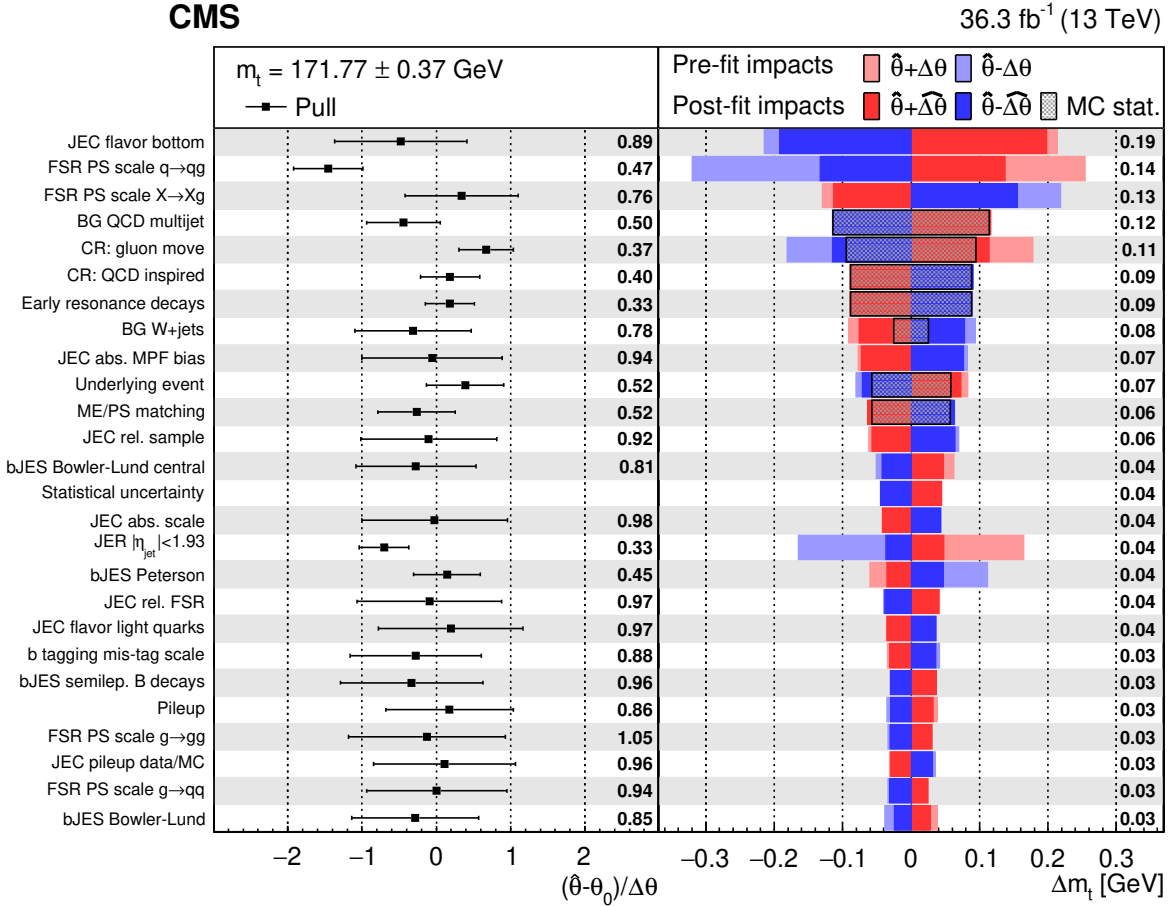


Figure 7: Measurement of m_t in the combined lepton+jets channel using the 5D set of observables and categories. The left plot shows the post-fit pulls on the most important nuisance parameters and the numbers quote the post-fit uncertainty in the nuisance parameter. The right plot shows their pre-fit (lighter colored bars) and post-fit impacts (darker colored bars) on m_t for up (red) and down (blue) variations. The post-fit impacts of systematic effects that are affected by the limited size of simulation samples include the contribution from the additional statistical nuisance parameters accounting for the effect. The size of the additional contribution from the statistical nuisance parameters is called MC stat. and shown as gray-dotted areas. The average of the post-fit impacts in GeV for up and down variations is printed on the right. The rows are sorted by the size of the averaged post-fit impact. The statistical uncertainty in m_t is depicted in the corresponding row.

matrix between the FSR PS scales for the different branching types. The result of this study is shown in Fig. 8. The final result strongly depends on the choice of the correlation coefficient between the FSR PS scales because of the significant deviation for the FSR PS scale of the $q \rightarrow qg$ branching from the default simulation. However, the assumption of strongly correlated FSR PS scale choices would also significantly reduce the overall uncertainty, as the impacts from the scale choice for gluon radiation from b quarks ($X \rightarrow Xg$) and light quarks ($q \rightarrow qg$) partially cancel. In addition, there is a tension between the measured nuisance parameter values for the different FSR PS scales, which disfavors a strong correlation. As there is only a small dependence on FSR PS scale correlations at low correlation coefficients ($\rho_{\text{FSR}} < 0.5$), and uncorrelated nuisance parameters for the FSR PS scales receive the least constraint from the fit to data, we assume uncorrelated FSR PS scales for this measurement.

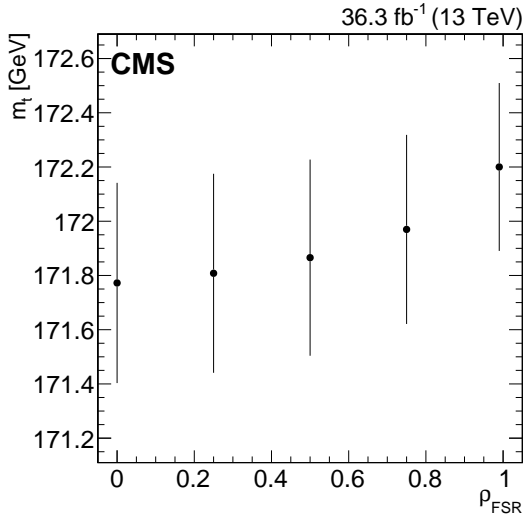


Figure 8: Dependence of the 5D result on the assumed correlation ρ_{FSR} between the FSR PS scales in the lepton+jets channel.

Most of the other nuisance parameters that show a strong post-fit constraint correspond to systematic uncertainties that are evaluated on independent samples of limited size. The small sample sizes are expected to bias these nuisances parameter and lead to too small uncertainties. Hence, the nuisance paramerts are accompanied by additional statistical nuisance parameters. A comparison of the pre-fit and post-fit impacts where the post-fit impacts include the impact of these statistical nuisance parameters shows that there is an only minimal constraint by the fit on the corresponding systematic uncertainties.

The largest constraint of a nuisance parameter without additional statistical nuisance parameters corresponds to the JER uncertainty. This is expected, as the energy resolution of jets from $t\bar{t}$ decays can be measured much better from the width of the m_W^{reco} distribution than by the extrapolation of the resolution measurement with dijet topologies at much higher transverse momenta [24].

Table 2 compares the measurements by the 2D and 5D methods with the previous result [13, 54] for the same data-taking period. The JEC uncertainties are grouped following the recommendations documented in Ref. [83]. The uncertainty in m_t for one source (row) in this table is evaluated from the covariance matrix of the ML fit by taking the square root of $\text{cov}(m_t, X)\text{cov}(X, X)^{-1}\text{cov}(X, m_t)$, where $\text{cov}(m_t, X)$, $\text{cov}(X, X)$, $\text{cov}(X, m_t)$ are the parts of the covariance matrix related to m_t or the set of nuisance parameters X contributing to the source, respectively. The statistical and calibration uncertainties are obtained differently by computing the partial covariance matrix on m_t where all other nuisance parameters are removed. The quadratic sum of all computed systematic uncertainties is larger than the uncertainty in m_t from the ML fit, as the sum ignores the post-fit correlations between the systematic uncertainty sources.

The 5D method is the only method that surpasses the strong reduction in the uncertainty in the JEC achieved by the previous analysis that determined m_t and in situ an overall jet energy scale factor (JSF). However, the measurement presented here also constrains the jet energy resolution uncertainty that was unaffected by the JSF. The new observables and additional events with a low P_{gof} reduce most modeling uncertainties, but lead to a slight increase in some experimental uncertainties. While the usage of weights for the PS variations removes the previously significant statistical component in the PS uncertainties, the introduction of separate PS scales

Table 2: Comparison of the uncertainty in the top quark mass in the previous measurement [13, 54] and the new 2D and 5D results in the lepton+jets channel.

	δm_t [GeV]		
	previous	2D	5D
<i>Experimental uncertainties</i>			
Method calibration	0.05	0.02	0.02
JEC	0.18	0.32	0.16
– Intercalibration	0.04	0.10	0.04
– MPFInSitu	0.07	0.15	0.07
– Uncorrelated	0.16	0.21	0.10
Jet energy resolution	0.12	0.12	0.05
b tagging	0.03	0.01	0.03
Lepton SFs and mom. scale		0.00	0.03
Pileup	0.05	0.00	0.03
Background	0.02	0.12	0.15
<i>Modeling uncertainties</i>			
JEC flavor	0.39	0.30	0.20
b-jet modeling	0.12	0.15	0.11
PDF	0.02	0.00	0.01
Renorm. and fact. scales	0.01	0.03	0.02
ME/PS matching	0.07	0.06	0.07
ME generator	0.20	—	—
ISR PS scale	0.07	0.01	0.01
FSR PS scale	0.13	0.37	0.21
Top quark p_T	0.01	0.06	0.00
Underlying event	0.07	0.09	0.04
Early resonance decays	0.07	0.13	0.09
CR modeling	0.31	0.15	0.15
Statistical	0.08	0.05	0.04
Total	0.63	0.52	0.37

leads to a large increase in the uncertainty in the FSR PS scale, despite the tight constraint on the corresponding nuisance parameters shown in Fig. 7.

The result presented here achieves a considerable improvement compared to all previously published top quark mass measurements. Hence, it supersedes the previously published measurement in this channel on the same data set [13]. The analysis shows the precision that is achievable from direct measurements of the top quark mass. As the uncertainty in the relationship of the direct measurement from simulation templates to a theoretically well-defined top quark mass is currently of similar size, the measurement should fuel further theoretical studies on the topic.

7 Summary

The mass of the top quark is measured using LHC proton-proton collision data collected in 2016 with the CMS detector at $\sqrt{s} = 13$ TeV, corresponding to an integrated luminosity of 36.3 fb^{-1} . The measurement uses a sample of $t\bar{t}$ events containing one isolated electron or muon and at least four jets in the final state. For each event, the mass is reconstructed from a kinematic

fit of the decay products to a $t\bar{t}$ hypothesis. A likelihood method is applied using up to four observables per event to extract the top quark mass and constrain the influences of systematic effects, which are included as nuisance parameters in the likelihood. The top quark mass is measured to be 171.77 ± 0.37 GeV. This result achieves a considerable improvement compared to all previously published top quark mass measurements and supersedes the previously published measurement in this channel on the same data set.

Acknowledgments

We congratulate our colleagues in the CERN accelerator departments for the excellent performance of the LHC and thank the technical and administrative staffs at CERN and at other CMS institutes for their contributions to the success of the CMS effort. In addition, we gratefully acknowledge the computing centers and personnel of the Worldwide LHC Computing Grid and other centers for delivering so effectively the computing infrastructure essential to our analyses. Finally, we acknowledge the enduring support for the construction and operation of the LHC, the CMS detector, and the supporting computing infrastructure provided by the following funding agencies: BMBWF and FWF (Austria); FNRS and FWO (Belgium); CNPq, CAPES, FAPERJ, FAPERGS, and FAPESP (Brazil); MES and BNSF (Bulgaria); CERN; CAS, MoST, and NSFC (China); MINCIENCIAS (Colombia); MSES and CSF (Croatia); RIF (Cyprus); SENESCYT (Ecuador); MoER, ERC PUT and ERDF (Estonia); Academy of Finland, MEC, and HIP (Finland); CEA and CNRS/IN2P3 (France); BMBF, DFG, and HGF (Germany); GSRI (Greece); NKFIH (Hungary); DAE and DST (India); IPM (Iran); SFI (Ireland); INFN (Italy); MSIP and NRF (Republic of Korea); MES (Latvia); LAS (Lithuania); MOE and UM (Malaysia); BUAP, CINVESTAV, CONACYT, LNS, SEP, and UASLP-FAI (Mexico); MOS (Montenegro); MBIE (New Zealand); PAEC (Pakistan); MES and NSC (Poland); FCT (Portugal); JINR (Dubna); MON, RosAtom, RAS, RFBR, and NRC KI (Russia); MESTD (Serbia); MCIN / AEI and PCTI (Spain); MOSTR (Sri Lanka); Swiss Funding Agencies (Switzerland); MST (Taipei); MH-ESI and NSTDA (Thailand); TUBITAK and TENMAK (Turkey); NASU (Ukraine); STFC (United Kingdom); DOE and NSF (USA).

Individuals have received support from the Marie-Curie program and the European Research Council and Horizon 2020 Grant, contract Nos. 675440, 724704, 752730, 758316, 765710, 824093, 884104, and COST Action CA16108 (European Union); the Leventis Foundation; the Alfred P. Sloan Foundation; the Alexander von Humboldt Foundation; the Belgian Federal Science Policy Office; the Fonds pour la Formation à la Recherche dans l’Industrie et dans l’Agriculture (FRIA-Belgium); the Agentschap voor Innovatie door Wetenschap en Technologie (IWT-Belgium); the F.R.S.-FNRS and FWO (Belgium) under the “Excellence of Science – EOS” – be.h project n. 30820817; the Beijing Municipal Science & Technology Commission, No. Z191100007219010; the Ministry of Education, Youth and Sports (MEYS) of the Czech Republic; the Hellenic Foundation for Research and Innovation (HFRI), Project Number 2288 (Greece); the Deutsche Forschungsgemeinschaft (DFG), under Germany’s Excellence Strategy – EXC 2121 “Quantum Universe” – 390833306, and under project number 400140256 - GRK2497; the Hungarian Academy of Sciences, the New National Excellence Program - ÚNKP, the NKFIH research grants K 124845, K 124850, K 128713, K 128786, K 129058, K 131991, K 133046, K 138136, K 143460, K 143477, 2020-2.2.1-ED-2021-00181, and TKP2021-NKTA-64 (Hungary); the Council of Science and Industrial Research, India; the Latvian Council of Science; the Ministry of Education and Science, project no. 2022/WK/14, and the National Science Center, contracts Opus 2021/41/B/ST2/01369 and 2021/43/B/ST2/01552 (Poland); the Fundação para a Ciência e a Tecnologia, grant CEECIND/01334/2018 (Portugal); the National Priorities Research Program by Qatar National Research Fund; the Ministry of Science and Higher Education, projects no.

0723-2020-0041 and no. FSWW-2020-0008 (Russia); MCIN/AEI/10.13039/501100011033, ERDF “a way of making Europe”, and the Programa Estatal de Fomento de la Investigación Científica y Técnica de Excelencia María de Maeztu, grant MDM-2017-0765 and Programa Severo Ochoa del Principado de Asturias (Spain); the Chulalongkorn Academic into Its 2nd Century Project Advancement Project, and the National Science, Research and Innovation Fund via the Program Management Unit for Human Resources & Institutional Development, Research and Innovation, grant B05F650021 (Thailand); the Kavli Foundation; the Nvidia Corporation; the SuperMicro Corporation; the Welch Foundation, contract C-1845; and the Weston Havens Foundation (USA).

References

- [1] CDF Collaboration, “Observation of top quark production in $\bar{p}p$ collisions”, *Phys. Rev. Lett.* **74** (1995) 2626, doi:10.1103/PhysRevLett.74.2626, arXiv:hep-ex/9503002.
- [2] D0 Collaboration, “Observation of the top quark”, *Phys. Rev. Lett.* **74** (1995) 2632, doi:10.1103/PhysRevLett.74.2632, arXiv:hep-ex/9503003.
- [3] G. Degrassi et al., “Higgs mass and vacuum stability in the standard model at NNLO”, *JHEP* **08** (2012) 1, doi:10.1007/JHEP08(2012)098, arXiv:1205.6497.
- [4] F. Bezrukov, M. Y. Kalmykov, B. A. Kniehl, and M. Shaposhnikov, “Higgs boson mass and new physics”, *JHEP* **10** (2012) 140, doi:10.1007/JHEP10(2012)140, arXiv:1205.2893.
- [5] The ALEPH, DELPHI, L3, and OPAL Collaborations and the LEP Electroweak Working Group, “Electroweak measurements in electron-positron collisions at W-boson-pair energies at LEP”, *Phys. Rept.* **532** (2013) 119, doi:10.1016/j.physrep.2013.07.004, arXiv:1302.3415.
- [6] M. Baak et al., “The electroweak fit of the standard model after the discovery of a new boson at the LHC”, *Eur. Phys. J. C* **72** (2012) 2205, doi:10.1140/epjc/s10052-012-2205-9, arXiv:1209.2716.
- [7] M. Baak et al., “The global electroweak fit at NNLO and prospects for the LHC and ILC”, *Eur. Phys. J. C* **74** (2014) 3046, doi:10.1140/epjc/s10052-014-3046-5, arXiv:1407.3792.
- [8] Particle Data Group, P. A. Zyla et al., “Review of particle physics”, *Prog. Theor. Exp. Phys.* **2020** (2020) 083C01, doi:10.1093/ptep/ptaa104.
- [9] CDF and D0 Collaborations, “Combination of CDF and D0 results on the mass of the top quark using up 9.7 fb^{-1} at the Tevatron”, FERMILAB-CONF-16-298-E, 2016. arXiv:1608.01881.
- [10] ATLAS Collaboration, “Measurement of the top quark mass in the $t\bar{t} \rightarrow \text{lepton+jets}$ channel from $\sqrt{s} = 8 \text{ TeV}$ ATLAS data and combination with previous results”, *Eur. Phys. J. C* **79** (2019) 290, doi:10.1140/epjc/s10052-019-6757-9, arXiv:1810.01772.

- [11] CMS Collaboration, “Measurement of the top quark mass using proton-proton data at $\sqrt{s} = 7$ and 8 TeV”, *Phys. Rev. D* **93** (2016) 072004, doi:10.1103/PhysRevD.93.072004, arXiv:1509.04044.
- [12] A. H. Hoang, “What is the top quark mass?”, *Ann. Rev. Nucl. Part. Sci.* **70** (2020) 225, doi:10.1146/annurev-nucl-101918-023530, arXiv:2004.12915.
- [13] CMS Collaboration, “Measurement of the top quark mass with lepton+jets final states using pp collisions at $\sqrt{s} = 13$ TeV”, *Eur. Phys. J. C* **78** (2018) 891, doi:10.1140/epjc/s10052-018-6332-9, arXiv:1805.01428.
- [14] DELPHI Collaboration, “Measurement of the mass and width of the W boson in e^+e^- collisions at $\sqrt{s} = 161\text{--}209$ GeV”, *Eur. Phys. J. C* **55** (2008) 1, doi:10.1140/epjc/s10052-008-0585-7, arXiv:0803.2534.
- [15] CMS Collaboration, “Measurement of the top-quark mass in $t\bar{t}$ events with lepton+jets final states in pp collisions at $\sqrt{s} = 7$ TeV”, *JHEP* **12** (2012) 105, doi:10.1007/JHEP12(2012)105, arXiv:1209.2319.
- [16] CMS Collaboration, “Extraction and validation of a new set of CMS PYTHIA8 tunes from underlying-event measurements”, *Eur. Phys. J. C* **80** (2020) 4, doi:10.1140/epjc/s10052-019-7499-4, arXiv:1903.12179.
- [17] E. Bols et al., “Jet flavour classification using DeepJet”, *JINST* **15** (2020) P12012, doi:10.1088/1748-0221/15/12/P12012, arXiv:2008.10519.
- [18] HEPData record for this analysis, 2023. doi:10.17182/hepdata.127993.
- [19] CMS Collaboration, “The CMS experiment at the CERN LHC”, *JINST* **3** (2008) S08004, doi:10.1088/1748-0221/3/08/S08004.
- [20] CMS Collaboration, “Technical proposal for the Phase-II upgrade of the Compact Muon Solenoid”, CMS Technical Proposal CERN-LHCC-2015-010, CMS-TDR-15-02, 2015.
- [21] CMS Collaboration, “Particle-flow reconstruction and global event description with the CMS detector”, *JINST* **12** (2017) P10003, doi:10.1088/1748-0221/12/10/P10003, arXiv:1706.04965.
- [22] M. Cacciari, G. P. Salam, and G. Soyez, “The anti- k_T jet clustering algorithm”, *JHEP* **04** (2008) 063, doi:10.1088/1126-6708/2008/04/063, arXiv:0802.1189.
- [23] M. Cacciari, G. P. Salam, and G. Soyez, “FastJet user manual”, *Eur. Phys. J. C* **72** (2012) 1896, doi:10.1140/epjc/s10052-012-1896-2, arXiv:1111.6097.
- [24] CMS Collaboration, “Jet energy scale and resolution in the CMS experiment in pp collisions at 8 TeV”, *JINST* **12** (2017) P02014, doi:10.1088/1748-0221/12/02/P02014, arXiv:1607.03663.
- [25] CMS Collaboration, “Identification of heavy-flavour jets with the CMS detector in pp collisions at 13 TeV”, *JINST* **13** (2018) P05011, doi:10.1088/1748-0221/13/05/P05011, arXiv:1712.07158.
- [26] CMS Collaboration, “Performance of the DeepJet b tagging algorithm using 41.9/fb of data from proton-proton collisions at 13 TeV with Phase 1 CMS detector”, CMS Detector Performance Note CMS-DP-2018-058, 2018.

- [27] CMS Collaboration, “Performance of missing transverse momentum reconstruction in proton-proton collisions at $\sqrt{s} = 13$ TeV using the CMS detector”, *JINST* **14** (2019) P07004, doi:[10.1088/1748-0221/14/07/P07004](https://doi.org/10.1088/1748-0221/14/07/P07004), arXiv:[1903.06078](https://arxiv.org/abs/1903.06078).
- [28] CMS Collaboration, “Electron and photon reconstruction and identification with the CMS experiment at the CERN LHC”, *JINST* **16** (2021) P05014, doi:[10.1088/1748-0221/16/05/P05014](https://doi.org/10.1088/1748-0221/16/05/P05014), arXiv:[2012.06888](https://arxiv.org/abs/2012.06888).
- [29] CMS Collaboration, “ECAL 2016 refined calibration and Run2 summary plots”, CMS Detector Performance Note CMS-DP-2020-021, 2020.
- [30] CMS Collaboration, “Performance of the CMS muon detector and muon reconstruction with proton-proton collisions at $\sqrt{s} = 13$ TeV”, *JINST* **13** (2018) P06015, doi:[10.1088/1748-0221/13/06/P06015](https://doi.org/10.1088/1748-0221/13/06/P06015), arXiv:[1804.04528](https://arxiv.org/abs/1804.04528).
- [31] CMS Collaboration, “Precision luminosity measurement in proton-proton collisions at $\sqrt{s} = 13$ TeV in 2015 and 2016 at CMS”, *Eur. Phys. J. C* **81** (2021) 800, doi:[10.1140/epjc/s10052-021-09538-2](https://doi.org/10.1140/epjc/s10052-021-09538-2), arXiv:[2104.01927](https://arxiv.org/abs/2104.01927).
- [32] CMS Collaboration, “The CMS trigger system”, *JINST* **12** (2017) P01020, doi:[10.1088/1748-0221/12/01/P01020](https://doi.org/10.1088/1748-0221/12/01/P01020), arXiv:[1609.02366](https://arxiv.org/abs/1609.02366).
- [33] P. Nason, “A new method for combining NLO QCD with shower Monte Carlo algorithms”, *JHEP* **11** (2004) 040, doi:[10.1088/1126-6708/2004/11/040](https://doi.org/10.1088/1126-6708/2004/11/040), arXiv:[hep-ph/0409146](https://arxiv.org/abs/hep-ph/0409146).
- [34] S. Frixione, P. Nason, and C. Oleari, “Matching NLO QCD computations with parton shower simulations: the POWHEG method”, *JHEP* **11** (2007) 070, doi:[10.1088/1126-6708/2007/11/070](https://doi.org/10.1088/1126-6708/2007/11/070), arXiv:[0709.2092](https://arxiv.org/abs/0709.2092).
- [35] S. Alioli, P. Nason, C. Oleari, and E. Re, “A general framework for implementing NLO calculations in shower Monte Carlo programs: the POWHEG BOX”, *JHEP* **06** (2010) 043, doi:[10.1007/JHEP06\(2010\)043](https://doi.org/10.1007/JHEP06(2010)043), arXiv:[1002.2581](https://arxiv.org/abs/1002.2581).
- [36] T. Sjöstrand et al., “An introduction to PYTHIA8.2”, *Comput. Phys. Commun.* **191** (2015) 159, doi:[10.1016/j.cpc.2015.01.024](https://doi.org/10.1016/j.cpc.2015.01.024), arXiv:[1410.3012](https://arxiv.org/abs/1410.3012).
- [37] J. Butterworth et al., “PDF4LHC recommendations for LHC Run II”, *J. Phys. G* **43** (2016) 023001, doi:[10.1088/0954-3899/43/2/023001](https://doi.org/10.1088/0954-3899/43/2/023001), arXiv:[1510.03865](https://arxiv.org/abs/1510.03865).
- [38] NNPDF Collaboration, “Parton distributions from high-precision collider data”, *Eur. Phys. J. C* **77** (2017) 663, doi:[10.1140/epjc/s10052-017-5199-5](https://doi.org/10.1140/epjc/s10052-017-5199-5), arXiv:[1706.00428](https://arxiv.org/abs/1706.00428).
- [39] S. Alioli, P. Nason, C. Oleari, and E. Re, “NLO single-top production matched with shower in POWHEG: s - and t -channel contributions”, *JHEP* **09** (2009) 111, doi:[10.1088/1126-6708/2009/09/111](https://doi.org/10.1088/1126-6708/2009/09/111), arXiv:[0907.4076](https://arxiv.org/abs/0907.4076). [Erratum: doi:[10.1007/JHEP02\(2010\)011](https://doi.org/10.1007/JHEP02(2010)011)].
- [40] E. Re, “Single-top Wt-channel production matched with parton showers using the POWHEG method”, *Eur. Phys. J. C* **71** (2011) 1547, doi:[10.1140/epjc/s10052-011-1547-z](https://doi.org/10.1140/epjc/s10052-011-1547-z), arXiv:[1009.2450](https://arxiv.org/abs/1009.2450).

- [41] J. Alwall et al., “The automated computation of tree-level and next-to-leading order differential cross sections, and their matching to parton shower simulations”, *JHEP* **07** (2014) 079, doi:[10.1007/JHEP07\(2014\)079](https://doi.org/10.1007/JHEP07(2014)079), arXiv:[1405.0301](https://arxiv.org/abs/1405.0301).
- [42] J. Alwall et al., “Comparative study of various algorithms for the merging of parton showers and matrix elements in hadronic collisions”, *Eur. Phys. J. C* **53** (2008) 473, doi:[10.1140/epjc/s10052-007-0490-5](https://doi.org/10.1140/epjc/s10052-007-0490-5), arXiv:[0706.2569](https://arxiv.org/abs/0706.2569).
- [43] R. Frederix and S. Frixione, “Merging meets matching in MC@NLO”, *JHEP* **12** (2012) 061, doi:[10.1007/JHEP12\(2012\)061](https://doi.org/10.1007/JHEP12(2012)061), arXiv:[1209.6215](https://arxiv.org/abs/1209.6215).
- [44] P. Skands, S. Carrazza, and J. Rojo, “Tuning PYTHIA8.1: the Monash 2013 tune”, *Eur. Phys. J. C* **74** (2014) 3024, doi:[10.1140/epjc/s10052-014-3024-y](https://doi.org/10.1140/epjc/s10052-014-3024-y), arXiv:[1404.5630](https://arxiv.org/abs/1404.5630).
- [45] GEANT4 Collaboration, “GEANT4—a simulation toolkit”, *Nucl. Instrum. Meth. A* **506** (2003) 250, doi:[10.1016/S0168-9002\(03\)01368-8](https://doi.org/10.1016/S0168-9002(03)01368-8).
- [46] M. Czakon and A. Mitov, “Top++: A program for the calculation of the top-pair cross-section at hadron colliders”, *Comput. Phys. Commun.* **185** (2014) 2930, doi:[10.1016/j.cpc.2014.06.021](https://doi.org/10.1016/j.cpc.2014.06.021), arXiv:[1112.5675](https://arxiv.org/abs/1112.5675).
- [47] Y. Li and F. Petriello, “Combining QCD and electroweak corrections to dilepton production in FEWZ”, *Phys. Rev. D* **86** (2012) 094034, doi:[10.1103/PhysRevD.86.094034](https://doi.org/10.1103/PhysRevD.86.094034), arXiv:[1208.5967](https://arxiv.org/abs/1208.5967).
- [48] M. Aliev et al., “HATHOR: HAdronic Top and Heavy quarks crOss section calculatoR”, *Comput. Phys. Commun.* **182** (2011) 1034, doi:[10.1016/j.cpc.2010.12.040](https://doi.org/10.1016/j.cpc.2010.12.040), arXiv:[1007.1327](https://arxiv.org/abs/1007.1327).
- [49] P. Kant et al., “HATHOR for single top-quark production: Updated predictions and uncertainty estimates for single top-quark production in hadronic collisions”, *Comput. Phys. Commun.* **191** (2015) 74, doi:[10.1016/j.cpc.2015.02.001](https://doi.org/10.1016/j.cpc.2015.02.001), arXiv:[1406.4403](https://arxiv.org/abs/1406.4403).
- [50] D0 Collaboration, “Direct measurement of the top quark mass at D0”, *Phys. Rev. D* **58** (1998) 052001, doi:[10.1103/PhysRevD.58.052001](https://doi.org/10.1103/PhysRevD.58.052001), arXiv:[hep-ex/9801025](https://arxiv.org/abs/hep-ex/9801025).
- [51] ATLAS Collaboration, “Measurement of the top quark mass in the $t\bar{t} \rightarrow$ dilepton channel from $\sqrt{s} = 8$ TeV ATLAS data”, *Phys. Lett. B* **761** (2016) 350, doi:[10.1016/j.physletb.2016.08.042](https://doi.org/10.1016/j.physletb.2016.08.042), arXiv:[1606.02179](https://arxiv.org/abs/1606.02179).
- [52] CMS Collaboration, “Measurement of the $t\bar{t}$ production cross section, the top quark mass, and the strong coupling constant using dilepton events in pp collisions at $\sqrt{s} = 13$ TeV”, *Eur. Phys. J. C* **79** (2019) 368, doi:[10.1140/epjc/s10052-019-6863-8](https://doi.org/10.1140/epjc/s10052-019-6863-8), arXiv:[1812.10505](https://arxiv.org/abs/1812.10505).
- [53] ATLAS Collaboration, “Measurement of the top quark mass in the $t\bar{t} \rightarrow$ lepton+jets and $t\bar{t} \rightarrow$ dilepton channels using $\sqrt{s} = 7$ TeV ATLAS data”, *Eur. Phys. J. C* **75** (2015) 330, doi:[10.1140/epjc/s10052-015-3544-0](https://doi.org/10.1140/epjc/s10052-015-3544-0), arXiv:[1503.05427](https://arxiv.org/abs/1503.05427).
- [54] CMS Collaboration, “Measurement of the top quark mass in the all-jets final state at $\sqrt{s} = 13$ TeV and combination with the lepton+jets channel”, *Eur. Phys. J. C* **79** (2019) 313, doi:[10.1140/epjc/s10052-019-6788-2](https://doi.org/10.1140/epjc/s10052-019-6788-2), arXiv:[1812.10534](https://arxiv.org/abs/1812.10534).

- [55] CMS Collaboration, “Jet energy scale and resolution performance with 13 TeV data collected by CMS in 2016–2018”, CMS Detector Performance Note CMS-DP-2020-019, 2020.
- [56] CMS Collaboration, “Measurement of the inelastic proton-proton cross section at $\sqrt{s} = 13$ TeV”, *JHEP* **07** (2018) 161, doi:10.1007/JHEP07(2018)161, arXiv:1802.02613.
- [57] CMS Collaboration, “Measurement of the t -channel single-top-quark production cross section and of the $|V_{tb}|$ CKM matrix element in pp collisions at $\sqrt{s} = 8$ TeV”, *JHEP* **06** (2014) 090, doi:10.1007/JHEP06(2014)090, arXiv:1403.7366.
- [58] CMS Collaboration, “Cross section measurement of t -channel single top quark production in pp collisions at $\sqrt{s} = 13$ TeV”, *Phys. Lett. B* **772** (2017) 752, doi:10.1016/j.physletb.2017.07.047, arXiv:1610.00678.
- [59] CMS Collaboration, “Measurement of the production cross section of a W boson in association with two b jets in pp collisions at $\sqrt{s} = 8$ TeV”, *Eur. Phys. J. C.* **77** (2017) 92, doi:10.1140/epjc/s10052-016-4573-z, arXiv:1608.07561.
- [60] CMS Collaboration, “Measurements of the associated production of a Z boson and b jets in pp collisions at $\sqrt{s} = 8$ TeV”, *Eur. Phys. J. C* **77** (2017) 751, doi:10.1140/epjc/s10052-017-5140-y, arXiv:1611.06507.
- [61] CMS Collaboration, “Measurement of the WZ production cross section in pp collisions at $\sqrt{s} = 13$ TeV”, *Phys. Lett. B* **766** (2017) 268, doi:10.1016/j.physletb.2017.01.011, arXiv:1607.06943.
- [62] CMS Collaboration, “Measurements of the $pp \rightarrow ZZ$ production cross section and the $Z \rightarrow 4\ell$ branching fraction, and constraints on anomalous triple gauge couplings at $\sqrt{s} = 13$ TeV”, *Eur. Phys. J. C* **78** (2018) 165, doi:10.1140/epjc/s10052-018-5567-9, arXiv:1709.08601.
- [63] T. Sjöstrand, S. Mrenna, and P. Z. Skands, “PYTHIA 6.4 physics and manual”, *JHEP* **05** (2006) 026, doi:10.1088/1126-6708/2006/05/026, arXiv:hep-ph/0603175.
- [64] M. Bähr et al., “Herwig++ physics and manual”, *Eur. Phys. J. C* **58** (2008) 639, doi:10.1140/epjc/s10052-008-0798-9, arXiv:0803.0883.
- [65] DELPHI Collaboration, “A study of the b-quark fragmentation function with the DELPHI detector at LEP I and an averaged distribution obtained at the Z pole”, *Eur. Phys. J. C* **71** (2011) 1557, doi:10.1140/epjc/s10052-011-1557-x, arXiv:1102.4748.
- [66] ALEPH Collaboration, “Study of the fragmentation of b quarks into B mesons at the Z peak”, *Phys. Lett. B* **512** (2001) 30, doi:10.1016/S0370-2693(01)00690-6, arXiv:hep-ex/0106051.
- [67] S. Dulat et al., “New parton distribution functions from a global analysis of quantum chromodynamics”, *Phys. Rev. D* **93** (2016) 033006, doi:10.1103/PhysRevD.93.033006, arXiv:1506.07443.
- [68] L. A. Harland-Lang, A. D. Martin, P. Motylinski, and R. S. Thorne, “Parton distributions in the LHC era: MMHT 2014 PDFs”, *Eur. Phys. J. C* **75** (2015) 204, doi:10.1140/epjc/s10052-015-3397-6, arXiv:1412.3989.

- [69] CMS Collaboration, “Investigations of the impact of the parton shower tuning in PYTHIA8 in the modelling of $t\bar{t}$ at $\sqrt{s} = 8$ and 13 TeV”, CMS Physics Analysis Summary CMS-PAS-TOP-16-021, 2016.
- [70] S. Mrenna and P. Skands, “Automated parton-shower variations in PYTHIA8”, *Phys. Rev. D* **94** (2016) 074005, doi:10.1103/PhysRevD.94.074005, arXiv:1605.08352.
- [71] M. Czakon, D. Heymes, and A. Mitov, “High-precision differential predictions for top-quark pairs at the LHC”, *Phys. Rev. Lett.* **116** (2016) 082003, doi:10.1103/PhysRevLett.116.082003, arXiv:1511.00549.
- [72] M. Czakon et al., “Top-pair production at the LHC through NNLO QCD and NLO EW”, *JHEP* **10** (2017) 186, doi:10.1007/JHEP10(2017)186, arXiv:1705.04105.
- [73] S. Catani et al., “Top-quark pair production at the LHC: Fully differential QCD predictions at NNLO”, *JHEP* **07** (2019) 100, doi:10.1007/JHEP07(2019)100, arXiv:1906.06535.
- [74] CMS Collaboration, “Measurement of differential cross sections for top quark pair production using the lepton+jets final state in proton-proton collisions at 13 TeV”, *Phys. Rev. D* **95** (2017) 092001, doi:10.1103/PhysRevD.95.092001, arXiv:1610.04191.
- [75] CMS Collaboration, “Measurement of normalized differential $t\bar{t}$ cross sections in the dilepton channel from pp collisions at $\sqrt{s} = 13$ TeV”, *JHEP* **04** (2018) 060, doi:10.1007/JHEP04(2018)060, arXiv:1708.07638.
- [76] J. R. Christiansen and P. Z. Skands, “String formation beyond leading colour”, *JHEP* **08** (2015) 003, doi:10.1007/JHEP08(2015)003, arXiv:1505.01681.
- [77] S. Argyropoulos and T. Sjöstrand, “Effects of color reconnection on $t\bar{t}$ final states at the LHC”, *JHEP* **11** (2014) 043, doi:10.1007/JHEP11(2014)043, arXiv:1407.6653.
- [78] CMS Collaboration, “CMS PYTHIA8 colour reconnection tunes based on underlying-event data”, *Eur. Phys. J. C* **83** (2023) 587, doi:10.1140/epjc/s10052-023-11630-8, arXiv:2205.02905.
- [79] W. Verkerke and D. P. Kirkby, “The RooFit toolkit for data modeling”, in *Proceedings of the 13th International Conference for Computing in High-Energy and Nuclear Physics (CHEP03)*. 2003. arXiv:physics/0306116. [eConf C0303241, MOLT007].
- [80] F. James and M. Roos, “Minuit: A system for function minimization and analysis of the parameter errors and correlations”, *Comput. Phys. Commun.* **10** (1975) 343, doi:10.1016/0010-4655(75)90039-9.
- [81] R. J. Barlow and C. Beeston, “Fitting using finite Monte Carlo samples”, *Comput. Phys. Commun.* **77** (1993) 219, doi:10.1016/0010-4655(93)90005-W.
- [82] J. S. Conway, “Incorporating nuisance parameters in likelihoods for multisource spectra”, in *PHYSTAT 2011*, p. 115. 2011. arXiv:1103.0354. doi:10.5170/CERN-2011-006.115.
- [83] ATLAS and CMS Collaborations, “Jet energy scale uncertainty correlations between ATLAS and CMS at 8 TeV”, ATL-PHYS-PUB-2015-049, CMS-PAS-JME-15-001, 2015.

A The CMS Collaboration

Yerevan Physics Institute, Yerevan, Armenia

A. Tumasyan¹ 

Institut für Hochenergiephysik, Vienna, Austria

W. Adam , J.W. Andrejkovic, T. Bergauer , S. Chatterjee , K. Damanakis , M. Dragicevic , A. Escalante Del Valle , P.S. Hussain , M. Jeitler² , N. Krammer , L. Lechner , D. Liko , I. Mikulec , P. Paulitsch, F.M. Pitters, J. Schieck² , R. Schöfbeck , D. Schwarz , M. Sonawane , S. Templ , W. Waltenberger , C.-E. Wulz² 

Universiteit Antwerpen, Antwerpen, Belgium

M.R. Darwish³ , T. Janssen , T. Kello⁴, H. Rejeb Sfar, P. Van Mechelen 

Vrije Universiteit Brussel, Brussel, Belgium

E.S. Bols , J. D'Hondt , A. De Moor , M. Delcourt , H. El Faham , S. Lowette , S. Moortgat , A. Morton , D. Müller , A.R. Sahasransu , S. Tavernier , W. Van Doninck, D. Vannerom 

Université Libre de Bruxelles, Bruxelles, Belgium

B. Clerbaux , G. De Lentdecker , L. Favart , D. Hohov , J. Jaramillo , K. Lee , M. Mahdavikhorrami , I. Makarenko , A. Malara , S. Paredes , L. Pétré , N. Postiau, L. Thomas , M. Vanden Bemden , C. Vander Velde , P. Vanlaer 

Ghent University, Ghent, Belgium

D. Dobur , J. Knolle , L. Lambrecht , G. Mestdach, C. Rendón, A. Samalan, K. Skovpen , M. Tytgat , N. Van Den Bossche , B. Vermassen, L. Wezenbeek 

Université Catholique de Louvain, Louvain-la-Neuve, Belgium

A. Benecke , G. Bruno , F. Bury , C. Caputo , P. David , C. Delaere , I.S. Donertas , A. Giannanco , K. Jaffel , Sa. Jain , V. Lemaitre, K. Mondal , A. Taliercio , T.T. Tran , P. Vischia , S. Wertz 

Centro Brasileiro de Pesquisas Fisicas, Rio de Janeiro, Brazil

G.A. Alves , E. Coelho , C. Hensel , A. Moraes , P. Rebello Teles 

Universidade do Estado do Rio de Janeiro, Rio de Janeiro, Brazil

W.L. Aldá Júnior , M. Alves Gallo Pereira , M. Barroso Ferreira Filho , H. Brandao Malbouisson , W. Carvalho , J. Chinellato⁵, E.M. Da Costa , G.G. Da Silveira⁶ , D. De Jesus Damiao , V. Dos Santos Sousa , S. Fonseca De Souza , J. Martins⁷ , C. Mora Herrera , K. Mota Amarilo , L. Mundim , H. Nogima , A. Santoro , S.M. Silva Do Amaral , A. Sznajder , M. Thiel , A. Vilela Pereira 

Universidade Estadual Paulista, Universidade Federal do ABC, São Paulo, Brazil

C.A. Bernardes⁶ , L. Calligaris , T.R. Fernandez Perez Tomei , E.M. Gregores , P.G. Mercadante , S.F. Novaes , Sandra S. Padula 

Institute for Nuclear Research and Nuclear Energy, Bulgarian Academy of Sciences, Sofia, Bulgaria

A. Aleksandrov , G. Antchev , R. Hadjiiska , P. Iaydjiev , M. Misheva , M. Rodozov, M. Shopova , G. Sultanov 

University of Sofia, Sofia, Bulgaria

A. Dimitrov , T. Ivanov , L. Litov , B. Pavlov , P. Petkov , A. Petrov , E. Shumka 

Instituto De Alta Investigación, Universidad de Tarapacá, Casilla 7 D, Arica, Chile

S. Thakur 

Beihang University, Beijing, China

T. Cheng , T. Javaid⁸ , M. Mittal , L. Yuan 

Department of Physics, Tsinghua University, Beijing, China

M. Ahmad , G. Bauer⁹, Z. Hu , S. Lezki , K. Yi^{9,10} 

Institute of High Energy Physics, Beijing, China

G.M. Chen⁸ , H.S. Chen⁸ , M. Chen⁸ , F. Iemmi , C.H. Jiang, A. Kapoor , H. Liao , Z.-A. Liu¹¹ , V. Milosevic , F. Monti , R. Sharma , J. Tao , J. Thomas-Wilsker , J. Wang , H. Zhang , J. Zhao

State Key Laboratory of Nuclear Physics and Technology, Peking University, Beijing, China

A. Agapitos , Y. An , Y. Ban , A. Levin , C. Li , Q. Li , X. Lyu, Y. Mao, S.J. Qian , X. Sun , D. Wang , J. Xiao , H. Yang

Sun Yat-Sen University, Guangzhou, China

M. Lu , Z. You 

University of Science and Technology of China, Hefei, China

N. Lu 

Institute of Modern Physics and Key Laboratory of Nuclear Physics and Ion-beam Application (MOE) - Fudan University, Shanghai, China

X. Gao⁴ , D. Leggat, H. Okawa , Y. Zhang 

Zhejiang University, Hangzhou, Zhejiang, China

Z. Lin , C. Lu , M. Xiao 

Universidad de Los Andes, Bogota, Colombia

C. Avila , D.A. Barbosa Trujillo, A. Cabrera , C. Florez , J. Fraga 

Universidad de Antioquia, Medellin, Colombia

J. Mejia Guisao , F. Ramirez , M. Rodriguez , J.D. Ruiz Alvarez 

University of Split, Faculty of Electrical Engineering, Mechanical Engineering and Naval Architecture, Split, Croatia

D. Giljanovic , N. Godinovic , D. Lelas , I. Puljak 

University of Split, Faculty of Science, Split, Croatia

Z. Antunovic, M. Kovac , T. Sculac 

Institute Rudjer Boskovic, Zagreb, Croatia

V. Brigljevic , B.K. Chitroda , D. Ferencek , S. Mishra , M. Roguljic , A. Starodumov¹² , T. Susa 

University of Cyprus, Nicosia, Cyprus

A. Attikis , K. Christoforou , M. Kolosova , S. Konstantinou , J. Mousa , C. Nicolaou, F. Ptochos , P.A. Razis , H. Rykaczewski, H. Saka , A. Stepennov

Charles University, Prague, Czech Republic

M. Finger¹² , M. Finger Jr.¹² , A. Kveton 

Escuela Politecnica Nacional, Quito, Ecuador

E. Ayala 

Universidad San Francisco de Quito, Quito, Ecuador

E. Carrera Jarrin 

Academy of Scientific Research and Technology of the Arab Republic of Egypt, Egyptian Network of High Energy Physics, Cairo, Egypt

H. Abdalla¹³ , Y. Assran^{14,15} 

Center for High Energy Physics (CHEP-FU), Fayoum University, El-Fayoum, Egypt

A. Lotfy , M.A. Mahmoud 

National Institute of Chemical Physics and Biophysics, Tallinn, Estonia

S. Bhowmik , R.K. Dewanjee , K. Ehataht , M. Kadastik, T. Lange , S. Nandan , C. Nielsen , J. Pata , M. Raidal , L. Tani , C. Veelken 

Department of Physics, University of Helsinki, Helsinki, Finland

P. Eerola , H. Kirschenmann , K. Osterberg , M. Voutilainen 

Helsinki Institute of Physics, Helsinki, Finland

S. Bharthuar , E. Brücken , F. Garcia , J. Havukainen , M.S. Kim , R. Kinnunen, T. Lampén , K. Lassila-Perini , S. Lehti , T. Lindén , M. Lotti, L. Martikainen , M. Myllymäki , J. Ott , M.m. Rantanen , H. Siikonen , E. Tuominen , J. Tuominiemi

Lappeenranta-Lahti University of Technology, Lappeenranta, Finland

P. Luukka , H. Petrow , T. Tuuva

IRFU, CEA, Université Paris-Saclay, Gif-sur-Yvette, France

C. Amendola , M. Besancon , F. Couderc , M. Dejardin , D. Denegri, J.L. Faure, F. Ferri , S. Ganjour , P. Gras , G. Hamel de Monchenault , V. Lohezic , J. Malcles , J. Rander, A. Rosowsky , M.Ö. Sahin , A. Savoy-Navarro¹⁶ , P. Simkina , M. Titov

Laboratoire Leprince-Ringuet, CNRS/IN2P3, Ecole Polytechnique, Institut Polytechnique de Paris, Palaiseau, France

C. Baldenegro Barrera , F. Beaudette , A. Buchot Perraguin , P. Busson , A. Cappati , C. Charlot , F. Damas , O. Davignon , B. Diab , G. Falmagne , B.A. Fontana Santos Alves , S. Ghosh , R. Granier de Cassagnac , A. Hakimi , B. Harikrishnan , G. Liu , J. Motta , M. Nguyen , C. Ochando , L. Portales , R. Salerno , U. Sarkar , J.B. Sauvan , Y. Sirois , A. Tarabini , E. Vernazza , A. Zabi , A. Zghiche

Université de Strasbourg, CNRS, IPHC UMR 7178, Strasbourg, France

J.-L. Agram¹⁷ , J. Andrea , D. Apparu , D. Bloch , G. Bourgatte , J.-M. Brom , E.C. Chabert , C. Collard , D. Darej, U. Goerlach , C. Grimault, A.-C. Le Bihan , P. Van Hove 

Institut de Physique des 2 Infinis de Lyon (IP2I), Villeurbanne, France

S. Beauceron , B. Blançon , G. Boudoul , A. Carle, N. Chanon , J. Choi , D. Contardo , P. Depasse , C. Dozen¹⁸ , H. El Mamouni, J. Fay , S. Gascon , M. Gouzevitch , G. Grenier , B. Ille , I.B. Laktineh, M. Lethuillier , L. Mirabito, S. Perries, L. Torterotot , M. Vander Donckt , P. Verdier , S. Viret

Georgian Technical University, Tbilisi, Georgia

D. Chokheli , I. Lomidze , Z. Tsamalaidze¹² 

RWTH Aachen University, I. Physikalisches Institut, Aachen, Germany

V. Botta , L. Feld , K. Klein , M. Lipinski , D. Meuser , A. Pauls , N. Röwert , M. Teroerde 

RWTH Aachen University, III. Physikalisches Institut A, Aachen, Germany

S. Diekmann [ID](#), A. Dodonova [ID](#), N. Eich [ID](#), D. Eliseev [ID](#), M. Erdmann [ID](#), P. Fackeldey [ID](#), D. Fasanella [ID](#), B. Fischer [ID](#), T. Hebbeker [ID](#), K. Hoepfner [ID](#), F. Ivone [ID](#), M.y. Lee [ID](#), L. Mastrolorenzo, M. Merschmeyer [ID](#), A. Meyer [ID](#), S. Mondal [ID](#), S. Mukherjee [ID](#), D. Noll [ID](#), A. Novak [ID](#), F. Nowotny, A. Pozdnyakov [ID](#), Y. Rath, W. Redjeb [ID](#), H. Reithler [ID](#), A. Schmidt [ID](#), S.C. Schuler, A. Sharma [ID](#), A. Stein [ID](#), F. Torres Da Silva De Araujo¹⁹ [ID](#), L. Vigilante, S. Wiedenbeck [ID](#), S. Zaleski

RWTH Aachen University, III. Physikalisches Institut B, Aachen, Germany

C. Dziwok [ID](#), G. Flügge [ID](#), W. Haj Ahmad²⁰ [ID](#), O. Hlushchenko, T. Kress [ID](#), A. Nowack [ID](#), O. Pooth [ID](#), A. Stahl [ID](#), T. Ziemons [ID](#), A. Zottz [ID](#)

Deutsches Elektronen-Synchrotron, Hamburg, Germany

H. Aarup Petersen [ID](#), M. Aldaya Martin [ID](#), P. Asmuss, S. Baxter [ID](#), M. Bayatmakou [ID](#), O. Behnke [ID](#), A. Bermúdez Martínez [ID](#), S. Bhattacharya [ID](#), A.A. Bin Anuar [ID](#), F. Blekman²¹ [ID](#), K. Borras²² [ID](#), D. Brunner [ID](#), A. Campbell [ID](#), A. Cardini [ID](#), C. Cheng, F. Colombina [ID](#), S. Consuegra Rodríguez [ID](#), G. Correia Silva [ID](#), M. De Silva [ID](#), L. Didukh [ID](#), G. Eckerlin, D. Eckstein [ID](#), L.I. Estevez Banos [ID](#), O. Filatov [ID](#), E. Gallo²¹ [ID](#), A. Geiser [ID](#), A. Giraldi [ID](#), G. Greau, A. Grohsjean [ID](#), V. Guglielmi [ID](#), M. Guthoff [ID](#), A. Jafari²³ [ID](#), N.Z. Jomhari [ID](#), B. Kaech [ID](#), M. Kasemann [ID](#), H. Kaveh [ID](#), C. Kleinwort [ID](#), R. Kogler [ID](#), M. Komm [ID](#), D. Krücker [ID](#), W. Lange, D. Leyva Pernia [ID](#), K. Lipka²⁴ [ID](#), W. Lohmann²⁵ [ID](#), R. Mankel [ID](#), I.-A. Melzer-Pellmann [ID](#), M. Mendizabal Morentin [ID](#), J. Metwally, A.B. Meyer [ID](#), G. Milella [ID](#), M. Mormile [ID](#), A. Mussgiller [ID](#), A. Nürnberg [ID](#), Y. Otarid, D. Pérez Adán [ID](#), A. Raspereza [ID](#), B. Ribeiro Lopes [ID](#), J. Rübenach, A. Saggio [ID](#), A. Saibel [ID](#), M. Savitskyi [ID](#), M. Scham^{26,22} [ID](#), V. Scheurer, S. Schnake²² [ID](#), P. Schütze [ID](#), C. Schwanenberger²¹ [ID](#), M. Shchedrolosiev [ID](#), R.E. Sosa Ricardo [ID](#), D. Stafford, N. Tonon[†] [ID](#), M. Van De Klundert [ID](#), F. Vazzoler [ID](#), A. Ventura Barroso [ID](#), R. Walsh [ID](#), D. Walter [ID](#), Q. Wang [ID](#), Y. Wen [ID](#), K. Wichmann, L. Wiens²² [ID](#), C. Wissing [ID](#), S. Wuchterl [ID](#), Y. Yang [ID](#), A. Zimmermann Castro Santos [ID](#)

University of Hamburg, Hamburg, Germany

A. Albrecht [ID](#), S. Albrecht [ID](#), M. Antonello [ID](#), S. Bein [ID](#), L. Benato [ID](#), M. Bonanomi [ID](#), P. Connor [ID](#), K. De Leo [ID](#), M. Eich, K. El Morabit [ID](#), F. Feindt, A. Fröhlich, C. Garbers [ID](#), E. Garutti [ID](#), M. Hajheidari, J. Haller [ID](#), A. Hinzmänn [ID](#), H.R. Jabusch [ID](#), G. Kasieczka [ID](#), P. Keicher, R. Klanner [ID](#), W. Korcari [ID](#), T. Kramer [ID](#), V. Kutzner [ID](#), F. Labe [ID](#), J. Lange [ID](#), A. Lobanov [ID](#), C. Matthies [ID](#), A. Mehta [ID](#), L. Moureaux [ID](#), M. Mrowietz, A. Nigmatova [ID](#), Y. Nissan, A. Paasch [ID](#), K.J. Pena Rodriguez [ID](#), T. Quadfasel [ID](#), M. Rieger [ID](#), O. Rieger, D. Savoiu [ID](#), J. Schindler [ID](#), P. Schleper [ID](#), M. Schröder [ID](#), J. Schwandt [ID](#), M. Sommerhalder [ID](#), H. Stadie [ID](#), G. Steinbrück [ID](#), A. Tews, M. Wolf [ID](#)

Karlsruher Institut fuer Technologie, Karlsruhe, Germany

S. Brommer [ID](#), M. Burkart, E. Butz [ID](#), R. Caspart [ID](#), T. Chwalek [ID](#), A. Dierlamm [ID](#), A. Droll, N. Faltermann [ID](#), M. Giffels [ID](#), J.O. Gosewisch, A. Gottmann [ID](#), F. Hartmann²⁷ [ID](#), M. Horzela [ID](#), U. Husemann [ID](#), M. Klute [ID](#), R. Koppenhöfer [ID](#), M. Link, A. Lintuluoto [ID](#), S. Maier [ID](#), S. Mitra [ID](#), Th. Müller [ID](#), M. Neukum, M. Oh [ID](#), G. Quast [ID](#), K. Rabbertz [ID](#), J. Rauser, M. Schnepf, I. Shvetsov [ID](#), H.J. Simonis [ID](#), N. Trevisani [ID](#), R. Ulrich [ID](#), J. van der Linden [ID](#), R.F. Von Cube [ID](#), M. Wassmer [ID](#), S. Wieland [ID](#), R. Wolf [ID](#), S. Wozniewski [ID](#), S. Wunsch, X. Zuo [ID](#)

Institute of Nuclear and Particle Physics (INPP), NCSR Demokritos, Aghia Paraskevi, Greece

G. Anagnostou, P. Assiouras [ID](#), G. Daskalakis [ID](#), A. Kyriakis, A. Stakia [ID](#)

National and Kapodistrian University of Athens, Athens, Greece

M. Diamantopoulou, D. Karasavvas, P. Kontaxakis , A. Manousakis-Katsikakis , A. Panagiotou, I. Papavergou , N. Saoulidou , K. Theofilatos , E. Tziaferi , K. Vellidis , I. Zisopoulos

National Technical University of Athens, Athens, Greece

G. Bakas , T. Chatzistavrou, K. Kousouris , I. Papakrivopoulos , G. Tsipolitis, A. Zacharopoulou

University of Ioánnina, Ioánnina, Greece

K. Adamidis, I. Bestintzanos, I. Evangelou , C. Foudas, P. Gianneios , C. Kamtsikis, P. Katsoulis, P. Kokkas , P.G. Kosmoglou Kioseoglou , N. Manthos , I. Papadopoulos , J. Strologas

MTA-ELTE Lendület CMS Particle and Nuclear Physics Group, Eötvös Loránd University, Budapest, Hungary

M. Csand , K. Farkas , M.M.A. Gadallah²⁸ , S. Lkcs²⁹ , P. Major , K. Mandal , G. Psztor , A.J. Rndl³⁰ , O. Surnyi , G.I. Veres

Wigner Research Centre for Physics, Budapest, Hungary

M. Bartk³¹ , G. Bencze, C. Hajdu , D. Horvath^{32,33} , F. Sikler , V. Veszpremi

Institute of Nuclear Research ATOMKI, Debrecen, Hungary

N. Beni , S. Czellar, J. Karancsi³¹ , J. Molnar, Z. Szillasi, D. Teyssier

Institute of Physics, University of Debrecen, Debrecen, Hungary

P. Raics, B. Ujvari³⁴

Karoly Robert Campus, MATE Institute of Technology, Gyongyos, Hungary

T. Csorgo³⁰ , F. Nemes³⁰ , T. Novak

Panjab University, Chandigarh, India

J. Babbar , S. Bansal , S.B. Beri, V. Bhatnagar , G. Chaudhary , S. Chauhan , N. Dhingra³⁵ , R. Gupta, A. Kaur , A. Kaur , H. Kaur , M. Kaur , S. Kumar , P. Kumari , M. Meena , K. Sandeep , T. Sheokand, J.B. Singh³⁶ , A. Singla , A. K. Virdi

University of Delhi, Delhi, India

A. Ahmed , A. Bhardwaj , A. Chhetri , B.C. Choudhary , A. Kumar , M. Naimuddin , K. Ranjan , S. Saumya

Saha Institute of Nuclear Physics, HBNI, Kolkata, India

S. Baradia , S. Barman³⁷ , S. Bhattacharya , D. Bhowmik, S. Dutta , S. Dutta, B. Gomber³⁸ , M. Maity³⁷, P. Palit , G. Saha , B. Sahu , S. Sarkar

Indian Institute of Technology Madras, Madras, India

P.K. Behera , S.C. Behera , P. Kalbhor , J.R. Komaragiri³⁹ , D. Kumar³⁹ , A. Muhammad , L. Panwar³⁹ , R. Pradhan , P.R. Pujahari , A. Sharma , A.K. Sikdar , P.C. Tiwari³⁹ , S. Verma

Bhabha Atomic Research Centre, Mumbai, India

K. Naskar⁴⁰

Tata Institute of Fundamental Research-A, Mumbai, India

T. Aziz, I. Das , S. Dugad, M. Kumar , G.B. Mohanty , P. Suryadevara

Tata Institute of Fundamental Research-B, Mumbai, India

S. Banerjee [ID](#), R. Chudasama [ID](#), M. Guchait [ID](#), S. Karmakar [ID](#), S. Kumar [ID](#), G. Majumder [ID](#), K. Mazumdar [ID](#), S. Mukherjee [ID](#), A. Thachayath [ID](#)

National Institute of Science Education and Research, An OCC of Homi Bhabha National Institute, Bhubaneswar, Odisha, India

S. Bahinipati⁴¹ [ID](#), A.K. Das, C. Kar [ID](#), P. Mal [ID](#), T. Mishra [ID](#), V.K. Muraleedharan Nair Bindhu⁴² [ID](#), A. Nayak⁴² [ID](#), P. Saha [ID](#), S.K. Swain [ID](#), D. Vats⁴² [ID](#)

Indian Institute of Science Education and Research (IISER), Pune, India

A. Alpana [ID](#), S. Dube [ID](#), B. Kansal [ID](#), A. Laha [ID](#), S. Pandey [ID](#), A. Rastogi [ID](#), S. Sharma [ID](#)

Isfahan University of Technology, Isfahan, Iran

H. Bakhshiansohi^{43,44} [ID](#), E. Khazaie⁴⁴ [ID](#), M. Zeinali⁴⁵ [ID](#)

Institute for Research in Fundamental Sciences (IPM), Tehran, Iran

S. Chenarani⁴⁶ [ID](#), S.M. Etesami [ID](#), M. Khakzad [ID](#), M. Mohammadi Najafabadi [ID](#)

University College Dublin, Dublin, Ireland

M. Grunewald [ID](#)

INFN Sezione di Bari^a, Università di Bari^b, Politecnico di Bari^c, Bari, Italy

M. Abbrescia^{a,b} [ID](#), R. Aly^{a,c,47} [ID](#), C. Aruta^{a,b} [ID](#), A. Colaleo^a [ID](#), D. Creanza^{a,c} [ID](#), N. De Filippis^{a,c} [ID](#), M. De Palma^{a,b} [ID](#), A. Di Florio^{a,b} [ID](#), W. Elmetenawee^{a,b} [ID](#), F. Errico^{a,b} [ID](#), L. Fiore^a [ID](#), G. Iaselli^{a,c} [ID](#), G. Maggi^{a,c} [ID](#), M. Maggi^a [ID](#), I. Margjeka^{a,b} [ID](#), V. Mastrapasqua^{a,b} [ID](#), S. My^{a,b} [ID](#), S. Nuzzo^{a,b} [ID](#), A. Pellecchia^{a,b} [ID](#), A. Pompili^{a,b} [ID](#), G. Pugliese^{a,c} [ID](#), R. Radogna^a [ID](#), D. Ramos^a [ID](#), A. Ranieri^a [ID](#), G. Selvaggi^{a,b} [ID](#), L. Silvestris^a [ID](#), F.M. Simone^{a,b} [ID](#), Ü. Sözbilir^a [ID](#), A. Stamerra^a [ID](#), R. Venditti^a [ID](#), P. Verwilligen^a [ID](#)

INFN Sezione di Bologna^a, Università di Bologna^b, Bologna, Italy

G. Abbiendi [ID](#), C. Battilana^{a,b} [ID](#), D. Bonacorsi^{a,b} [ID](#), L. Borgonovi^a [ID](#), R. Campanini^{a,b} [ID](#), P. Capiluppi^{a,b} [ID](#), A. Castro^{a,b} [ID](#), F.R. Cavallo^a [ID](#), C. Ciocca^a [ID](#), M. Cuffiani^{a,b} [ID](#), G.M. Dallavalle^a [ID](#), T. Diotalevi^{a,b} [ID](#), F. Fabbri^a [ID](#), A. Fanfani^{a,b} [ID](#), P. Giacomelli^a [ID](#), L. Giommi^{a,b} [ID](#), C. Grandi^a [ID](#), L. Guiducci^{a,b} [ID](#), S. Lo Meo^{a,48} [ID](#), L. Lunerti^{a,b} [ID](#), S. Marcellini^a [ID](#), G. Masetti^a [ID](#), F.L. Navarreria^{a,b} [ID](#), A. Perrotta^a [ID](#), F. Primavera^{a,b} [ID](#), A.M. Rossi^{a,b} [ID](#), T. Rovelli^{a,b} [ID](#), G.P. Siroli^{a,b} [ID](#)

INFN Sezione di Catania^a, Università di Catania^b, Catania, Italy

S. Costa^{a,b,49} [ID](#), A. Di Mattia^a [ID](#), R. Potenza^{a,b} [ID](#), A. Tricomi^{a,b,49} [ID](#), C. Tuve^{a,b} [ID](#)

INFN Sezione di Firenze^a, Università di Firenze^b, Firenze, Italy

G. Barbagli^a [ID](#), G. Bardelli^{a,b} [ID](#), B. Camaiani^{a,b} [ID](#), A. Cassese^a [ID](#), R. Ceccarelli^{a,b} [ID](#), V. Ciulli^{a,b} [ID](#), C. Civinini^a [ID](#), R. D'Alessandro^{a,b} [ID](#), E. Focardi^{a,b} [ID](#), G. Latino^{a,b} [ID](#), P. Lenzi^{a,b} [ID](#), M. Lizzo^{a,b} [ID](#), M. Meschini^a [ID](#), S. Paoletti^a [ID](#), R. Seidita^{a,b} [ID](#), G. Sguazzoni^a [ID](#), L. Viliani^a [ID](#)

INFN Laboratori Nazionali di Frascati, Frascati, Italy

L. Benussi [ID](#), S. Bianco [ID](#), S. Meola⁵⁰ [ID](#), D. Piccolo [ID](#)

INFN Sezione di Genova^a, Università di Genova^b, Genova, Italy

M. Bozzo^{a,b} [ID](#), P. Chatagnon^a [ID](#), F. Ferro^a [ID](#), E. Robutti^a [ID](#), S. Tosi^{a,b} [ID](#)

INFN Sezione di Milano-Bicocca^a, Università di Milano-Bicocca^b, Milano, Italy

A. Benaglia^a [ID](#), G. Boldrini^a [ID](#), F. Brivio^{a,b} [ID](#), F. Cetorelli^{a,b} [ID](#), F. De Guio^{a,b} [ID](#), M.E. Dinardo^{a,b} [ID](#), P. Dini^a [ID](#), S. Gennai^a [ID](#), A. Ghezzi^{a,b} [ID](#), P. Govoni^{a,b} [ID](#), L. Guzzi^{a,b} [ID](#)

M.T. Lucchini^{a,b} , M. Malberti^a , S. Malvezzi^a , A. Massironi^a , D. Menasce^a , L. Moroni^a , M. Paganoni^{a,b} , D. Pedrini^a , B.S. Pinolini^a, S. Ragazzi^{a,b} , N. Redaelli^a , T. Tabarelli de Fatis^{a,b} , D. Zuolo^{a,b}

INFN Sezione di Napoli^a, Università di Napoli 'Federico II'^b, Napoli, Italy; Università della Basilicata^c, Potenza, Italy; Università G. Marconi^d, Roma, Italy

S. Buontempo^a , F. Carnevali^{a,b}, N. Cavallo^{a,c} , A. De Iorio^{a,b} , F. Fabozzi^{a,c} , A.O.M. Iorio^{a,b} , L. Lista^{a,b,51} , P. Paoluccia^{a,27} , B. Rossi^a , C. Sciacca^{a,b} 

INFN Sezione di Padova^a, Università di Padova^b, Padova, Italy; Università di Trento^c, Trento, Italy

P. Azzi^a , N. Bacchetta^{a,52} , A. Bergnoli^a , M. Biasotto^{a,53} , D. Bisello^{a,b} , P. Bortignon^a , A. Bragagnolo^{a,b} , R. Carlin^{a,b} , P. Checchia^a , T. Dorigo^a , F. Gasparini^{a,b} , G. Grossi^a, L. Layer^{a,54}, E. Lusiani^a , M. Margoni^{a,b} , A.T. Meneguzzo^{a,b} , J. Pazzini^{a,b} , P. Ronchese^{a,b} , R. Rossin^{a,b} , F. Simonetto^{a,b} , G. Strong^a , M. Tosi^{a,b} , H. Yarar^{a,b}, P. Zotto^{a,b} , A. Zucchetta^{a,b} , G. Zumerle^{a,b}

INFN Sezione di Pavia^a, Università di Pavia^b, Pavia, Italy

S. Abu Zeid^{a,55} , C. Aimè^{a,b} , A. Braghieri^a , S. Calzaferri^{a,b} , D. Fiorina^{a,b} , P. Montagna^{a,b} , V. Re^a , C. Riccardi^{a,b} , P. Salvini^a , I. Vai^a , P. Vitulo^{a,b} 

INFN Sezione di Perugia^a, Università di Perugia^b, Perugia, Italy

P. Asenov^{a,56} , G.M. Bilei^a , D. Ciangottini^{a,b} , L. Fanò^{a,b} , M. Magherini^{a,b} , G. Mantovani^{a,b}, V. Mariani^{a,b} , M. Menichelli^a , F. Moscatelli^{a,56} , A. Piccinelli^{a,b} , M. Presilla^{a,b} , A. Rossi^{a,b} , A. Santocchia^{a,b} , D. Spiga^a , T. Tedeschi^{a,b}

INFN Sezione di Pisa^a, Università di Pisa^b, Scuola Normale Superiore di Pisa^c, Pisa, Italy; Università di Siena^d, Siena, Italy

P. Azzurri^a , G. Bagliesi^a , V. Bertacchi^{a,c} , R. Bhattacharya^a , L. Bianchini^{a,b} , T. Boccali^a , E. Bossini^{a,b} , D. Bruschini^{a,c} , R. Castaldi^a , M.A. Ciocci^{a,b} , V. D'Amante^{a,d} , R. Dell'Orso^a , M.R. Di Domenico^{a,d} , S. Donato^a , A. Giassi^a , F. Ligabue^{a,c} , G. Mandorlia^{a,c} , D. Matos Figueiredo^a , A. Messineo^{a,b} , M. Musich^{a,b} , F. Palla^a , S. Parolia^a , G. Ramirez-Sanchez^{a,c} , A. Rizzi^{a,b} , G. Rolandi^{a,c} , S. Roy Chowdhury^a , T. Sarkar^a , A. Scribano^a , N. Shafiei^{a,b} , P. Spagnolo^a , R. Tenchini^a , G. Tonelli^{a,b} , N. Turini^{a,d} , A. Venturi^a , P.G. Verdini^a

INFN Sezione di Roma^a, Sapienza Università di Roma^b, Roma, Italy

P. Barria^a , M. Campana^{a,b} , F. Cavallari^a , D. Del Re^{a,b} , E. Di Marco^a , M. Diemoz^a , E. Longo^{a,b} , P. Meridiani^a , G. Organtini^{a,b} , F. Pandolfi^a , R. Paramatti^{a,b} , C. Quaranta^{a,b} , S. Rahatlou^{a,b} , C. Rovelli^a , F. Santanastasio^{a,b} , L. Soffi^a , R. Tramontano^{a,b}

INFN Sezione di Torino^a, Università di Torino^b, Torino, Italy; Università del Piemonte Orientale^c, Novara, Italy

N. Amapane^{a,b} , R. Arcidiacono^{a,c} , S. Argiro^{a,b} , M. Arneodo^{a,c} , N. Bartosik^a , R. Bellan^{a,b} , A. Bellora^{a,b} , C. Biino^a , N. Cartiglia^a , M. Costa^{a,b} , R. Covarelli^{a,b} , N. Demaria^a , M. Grippo^{a,b} , B. Kiani^{a,b} , F. Legger^a , C. Mariotti^a , S. Maselli^a , A. Mecca^{a,b} , E. Migliore^{a,b} , E. Monteil^{a,b} , M. Monteno^a , R. Mulargia^a , M.M. Obertino^{a,b} , G. Ortona^a , L. Pacher^{a,b} , N. Pastrone^a , M. Pelliccioni^a , M. Ruspa^{a,c} , K. Shchelina^a , F. Siviero^{a,b} , V. Sola^a , A. Solano^{a,b} , D. Soldi^{a,b} , A. Staiano^a , M. Tornago^{a,b} , D. Trocino^a , G. Umoret^{a,b} , A. Vagnerini^{a,b}

INFN Sezione di Trieste^a, Università di Trieste^b, Trieste, Italy

S. Belforte^a , V. Candelise^{a,b} , M. Casarsa^a , F. Cossutti^a , A. Da Rold^{a,b} , G. Della Ricca^{a,b} , G. Sorrentino^{a,b} 

Kyungpook National University, Daegu, Korea

S. Dogra , C. Huh , B. Kim , D.H. Kim , G.N. Kim , J. Kim, J. Lee , S.W. Lee , C.S. Moon , Y.D. Oh , S.I. Pak , M.S. Ryu , S. Sekmen , Y.C. Yang

Chonnam National University, Institute for Universe and Elementary Particles, Kwangju, Korea

H. Kim , D.H. Moon 

Hanyang University, Seoul, Korea

E. Asilar , T.J. Kim , J. Park 

Korea University, Seoul, Korea

S. Choi , S. Han, B. Hong , K. Lee, K.S. Lee , J. Lim, J. Park, S.K. Park, J. Yoo 

Kyung Hee University, Department of Physics, Seoul, Korea

J. Goh 

Sejong University, Seoul, Korea

H. S. Kim , Y. Kim, S. Lee

Seoul National University, Seoul, Korea

J. Almond, J.H. Bhyun, J. Choi , S. Jeon , J. Kim , J.S. Kim, S. Ko , H. Kwon , H. Lee , S. Lee, B.H. Oh , S.B. Oh , H. Seo , U.K. Yang, I. Yoon

University of Seoul, Seoul, Korea

W. Jang , D.Y. Kang, Y. Kang , D. Kim , S. Kim , B. Ko, J.S.H. Lee , Y. Lee , J.A. Merlin, I.C. Park , Y. Roh, D. Song, I.J. Watson , S. Yang 

Yonsei University, Department of Physics, Seoul, Korea

S. Ha , H.D. Yoo 

Sungkyunkwan University, Suwon, Korea

M. Choi , M.R. Kim , H. Lee, Y. Lee , Y. Lee , I. Yu 

College of Engineering and Technology, American University of the Middle East (AUM), Dasman, Kuwait

T. Beyrouty, Y. Maghrbi 

Riga Technical University, Riga, Latvia

K. Dreimanis , G. Pikurs, A. Potrebko , M. Seidel , V. Veckalns 

Vilnius University, Vilnius, Lithuania

M. Ambrozas , A. Carvalho Antunes De Oliveira , A. Juodagalvis , A. Rinkevicius , G. Tamulaitis 

National Centre for Particle Physics, Universiti Malaya, Kuala Lumpur, Malaysia

N. Bin Norjoharuddeen , S.Y. Hoh⁵⁷ , I. Yusuff⁵⁷ , Z. Zolkapli

Universidad de Sonora (UNISON), Hermosillo, Mexico

J.F. Benitez , A. Castaneda Hernandez , H.A. Encinas Acosta, L.G. Gallegos Maríñez, M. León Coello , J.A. Murillo Quijada , A. Sehrawat , L. Valencia Palomo 

Centro de Investigacion y de Estudios Avanzados del IPN, Mexico City, Mexico

G. Ayala , H. Castilla-Valdez , I. Heredia-De La Cruz⁵⁸ , R. Lopez-Fernandez 

C.A. Mondragon Herrera, D.A. Perez Navarro , A. Sánchez Hernández 

Universidad Iberoamericana, Mexico City, Mexico

C. Oropeza Barrera , F. Vazquez Valencia 

Benemerita Universidad Autonoma de Puebla, Puebla, Mexico

I. Pedraza , H.A. Salazar Ibarguen , C. Uribe Estrada 

University of Montenegro, Podgorica, Montenegro

I. Bubanja, J. Mijuskovic⁵⁹ , N. Raicevic 

National Centre for Physics, Quaid-I-Azam University, Islamabad, Pakistan

A. Ahmad , M.I. Asghar, A. Awais , M.I.M. Awan, M. Gul , H.R. Hoorani , W.A. Khan , M. Shoaib , M. Waqas 

AGH University of Krakow, Faculty of Computer Science, Electronics and Telecommunications, Krakow, Poland

V. Avati, L. Grzanka , M. Malawski 

National Centre for Nuclear Research, Swierk, Poland

H. Bialkowska , M. Bluj , B. Boimska , M. Górski , M. Kazana , M. Szleper , P. Zalewski 

Institute of Experimental Physics, Faculty of Physics, University of Warsaw, Warsaw, Poland

K. Bunkowski , K. Doroba , A. Kalinowski , M. Konecki , J. Krolikowski 

Laboratório de Instrumentação e Física Experimental de Partículas, Lisboa, Portugal

M. Araujo , P. Bargassa , D. Bastos , A. Boletti , P. Faccioli , M. Gallinaro , J. Hollar , N. Leonardo , T. Niknejad , M. Pisano , J. Seixas , J. Varela 

VINCA Institute of Nuclear Sciences, University of Belgrade, Belgrade, Serbia

P. Adzic⁶⁰ , M. Dordevic , P. Milenovic , J. Milosevic 

Centro de Investigaciones Energéticas Medioambientales y Tecnológicas (CIEMAT), Madrid, Spain

M. Aguilar-Benitez, J. Alcaraz Maestre , A. Álvarez Fernández , M. Barrio Luna, Cristina F. Bedoya , C.A. Carrillo Montoya , M. Cepeda , M. Cerrada , N. Colino , B. De La Cruz , A. Delgado Peris , D. Fernández Del Val , J.P. Fernández Ramos , J. Flix , M.C. Fouz , O. Gonzalez Lopez , S. Goy Lopez , J.M. Hernandez , M.I. Josa , J. León Holgado , D. Moran , C. Perez Dengra , A. Pérez-Calero Yzquierdo , J. Puerta Pelayo , I. Redondo , D.D. Redondo Ferrero , L. Romero, S. Sánchez Navas , J. Sastre , L. Urda Gómez , J. Vazquez Escobar , C. Willmott

Universidad Autónoma de Madrid, Madrid, Spain

J.F. de Trocóniz 

Universidad de Oviedo, Instituto Universitario de Ciencias y Tecnologías Espaciales de Asturias (ICTEA), Oviedo, Spain

B. Alvarez Gonzalez , J. Cuevas , J. Fernandez Menendez , S. Folgueras , I. Gonzalez Caballero , J.R. González Fernández , E. Palencia Cortezon , C. Ramón Álvarez , V. Rodríguez Bouza , A. Soto Rodríguez , A. Trapote , C. Vico Villalba 

Instituto de Física de Cantabria (IFCA), CSIC-Universidad de Cantabria, Santander, Spain

J.A. Brochero Cifuentes , I.J. Cabrillo , A. Calderon , J. Duarte Campderros , M. Fernandez , C. Fernandez Madrazo , A. García Alonso, G. Gomez , C. Lasosa García , C. Martinez Rivero , P. Martinez Ruiz del Arbol , F. Matorras , P. Matorras Cuevas 

J. Piedra Gomez [ID](#), C. Prieels, A. Ruiz-Jimeno [ID](#), L. Scodellaro [ID](#), I. Vila [ID](#), J.M. Vizan Garcia [ID](#)

University of Colombo, Colombo, Sri Lanka

M.K. Jayananda [ID](#), B. Kailasapathy⁶¹ [ID](#), D.U.J. Sonnadara [ID](#), D.D.C. Wickramarathna [ID](#)

University of Ruhuna, Department of Physics, Matara, Sri Lanka

W.G.D. Dharmaratna⁶² [ID](#), K. Liyanage [ID](#), N. Perera [ID](#), N. Wickramage [ID](#)

CERN, European Organization for Nuclear Research, Geneva, Switzerland

D. Abbaneo [ID](#), J. Alimena [ID](#), E. Auffray [ID](#), G. Auzinger [ID](#), J. Baechler, P. Baillon[†], D. Barney [ID](#), J. Bendavid [ID](#), M. Bianco [ID](#), B. Bilin [ID](#), A. Bocci [ID](#), E. Brondolin [ID](#), C. Caillol [ID](#), T. Camporesi [ID](#), G. Cerminara [ID](#), N. Chernyavskaya [ID](#), S.S. Chhibra [ID](#), S. Choudhury, M. Cipriani [ID](#), L. Cristella [ID](#), D. d'Enterria [ID](#), A. Dabrowski [ID](#), A. David [ID](#), A. De Roeck [ID](#), M.M. Defranchis [ID](#), M. Deile [ID](#), M. Dobson [ID](#), M. Dünser [ID](#), N. Dupont, F. Fallavollita⁶³, A. Florent [ID](#), L. Forthomme [ID](#), G. Franzoni [ID](#), W. Funk [ID](#), S. Ghosh [ID](#), S. Giani, D. Gigi, K. Gill [ID](#), F. Glege [ID](#), L. Gouskos [ID](#), E. Govorkova [ID](#), M. Haranko [ID](#), J. Hegeman [ID](#), V. Innocente [ID](#), T. James [ID](#), P. Janot [ID](#), J. Kaspar [ID](#), J. Kieseler [ID](#), N. Kratochwil [ID](#), S. Laurila [ID](#), P. Lecoq [ID](#), E. Leutgeb [ID](#), C. Lourenço [ID](#), B. Maier [ID](#), L. Malgeri [ID](#), M. Mannelli [ID](#), A.C. Marini [ID](#), F. Meijers [ID](#), S. Mersi [ID](#), E. Meschi [ID](#), F. Moortgat [ID](#), M. Mulders [ID](#), S. Orfanelli, L. Orsini, F. Pantaleo [ID](#), E. Perez, M. Peruzzi [ID](#), A. Petrilli [ID](#), G. Petrucciani [ID](#), A. Pfeiffer [ID](#), M. Pierini [ID](#), D. Piparo [ID](#), M. Pitt [ID](#), H. Qu [ID](#), T. Quast, D. Rabady [ID](#), A. Racz, G. Reales Gutierrez, M. Rovere [ID](#), H. Sakulin [ID](#), J. Salfeld-Nebgen [ID](#), S. Scarfi [ID](#), M. Selvaggi [ID](#), A. Sharma [ID](#), P. Silva [ID](#), P. Sphicas⁶⁴ [ID](#), A.G. Stahl Leiton [ID](#), S. Summers [ID](#), K. Tatar [ID](#), V.R. Tavolaro [ID](#), D. Treille [ID](#), P. Tropea [ID](#), A. Tsirou, J. Wanczyk⁶⁵ [ID](#), K.A. Wozniak [ID](#), W.D. Zeuner

Paul Scherrer Institut, Villigen, Switzerland

L. Caminada⁶⁶ [ID](#), A. Ebrahimi [ID](#), W. Erdmann [ID](#), R. Horisberger [ID](#), Q. Ingram [ID](#), H.C. Kaestli [ID](#), D. Kotlinski [ID](#), C. Lange [ID](#), M. Missiroli⁶⁶ [ID](#), L. Noehte⁶⁶ [ID](#), T. Rohe [ID](#)

ETH Zurich - Institute for Particle Physics and Astrophysics (IPA), Zurich, Switzerland

T.K. Arrestad [ID](#), K. Androsov⁶⁵ [ID](#), M. Backhaus [ID](#), P. Berger, A. Calandri [ID](#), K. Datta [ID](#), A. De Cosa [ID](#), G. Dissertori [ID](#), M. Dittmar, M. Donegà [ID](#), F. Eble [ID](#), M. Galli [ID](#), K. Gedia [ID](#), F. Glessgen [ID](#), T.A. Gómez Espinosa [ID](#), C. Grab [ID](#), D. Hits [ID](#), W. Lustermann [ID](#), A.-M. Lyon [ID](#), R.A. Manzoni [ID](#), L. Marchese [ID](#), C. Martin Perez [ID](#), A. Mascellani⁶⁵ [ID](#), F. Nessi-Tedaldi [ID](#), J. Niedziela [ID](#), F. Pauss [ID](#), V. Perovic [ID](#), S. Pigazzini [ID](#), M.G. Ratti [ID](#), M. Reichmann [ID](#), C. Reissel [ID](#), T. Reitenspiess [ID](#), B. Ristic [ID](#), F. Riti [ID](#), D. Ruini, D.A. Sanz Becerra [ID](#), J. Steggemann⁶⁵ [ID](#), D. Valsecchi²⁷ [ID](#), R. Wallny [ID](#)

Universität Zürich, Zurich, Switzerland

C. Amsler⁶⁷ [ID](#), P. Bärtschi [ID](#), C. Botta [ID](#), D. Brzhechko, M.F. Canelli [ID](#), K. Cormier [ID](#), A. De Wit [ID](#), R. Del Burgo, J.K. Heikkilä [ID](#), M. Huwiler [ID](#), W. Jin [ID](#), A. Jofrehei [ID](#), B. Kilminster [ID](#), S. Leontsinis [ID](#), S.P. Liechti [ID](#), A. Macchiolo [ID](#), P. Meiring [ID](#), V.M. Mikuni [ID](#), U. Molinatti [ID](#), I. Neutelings [ID](#), A. Reimers [ID](#), P. Robmann, S. Sanchez Cruz [ID](#), K. Schweiger [ID](#), M. Senger [ID](#), Y. Takahashi [ID](#)

National Central University, Chung-Li, Taiwan

C. Adloff⁶⁸, C.M. Kuo, W. Lin, P.K. Rout [ID](#), S.S. Yu [ID](#)

National Taiwan University (NTU), Taipei, Taiwan

L. Ceard, Y. Chao [ID](#), K.F. Chen [ID](#), P.s. Chen, H. Cheng [ID](#), W.-S. Hou [ID](#), R. Khurana, G. Kole [ID](#), Y.y. Li [ID](#), R.-S. Lu [ID](#), E. Paganis [ID](#), A. Psallidas, A. Steen [ID](#), H.y. Wu, E. Yazgan [ID](#), P.r. Yu

Chulalongkorn University, Faculty of Science, Department of Physics, Bangkok, Thailand

C. Asawatangtrakuldee , N. Srimanobhas , V. Wachirapusitanand 

Çukurova University, Physics Department, Science and Art Faculty, Adana, Turkey

D. Agyel , F. Boran , Z.S. Demiroglu , F. Dolek , I. Dumanoglu⁶⁹ , E. Eskut , Y. Guler⁷⁰ , E. Gurpinar Guler⁷⁰ , C. Isik , O. Kara, A. Kayis Topaksu , U. Kiminsu , G. Onengut , K. Ozdemir⁷¹ , A. Polatoz , A.E. Simsek , B. Tali⁷² , U.G. Tok , S. Turkcapar , E. Uslan , I.S. Zorbakir

Middle East Technical University, Physics Department, Ankara, Turkey

G. Karapinar⁷³ , K. Ocalan⁷⁴ , M. Yalvac⁷⁵ 

Bogazici University, Istanbul, Turkey

B. Akgun , I.O. Atakisi , E. Gürmez , M. Kaya⁷⁶ , O. Kaya⁷⁷ , S. Tekten⁷⁸ 

Istanbul Technical University, Istanbul, Turkey

A. Cakir , K. Cankocak⁶⁹ , Y. Komurcu , S. Sen⁷⁹ 

Istanbul University, Istanbul, Turkey

O. Aydilek , S. Cerci⁷² , B. Hacisahinoglu , I. Hos⁸⁰ , B. Isildak⁸¹ , B. Kaynak , S. Ozkorucuklu , C. Simsek , D. Sunar Cerci⁷² 

Institute for Scintillation Materials of National Academy of Science of Ukraine, Kharkiv, Ukraine

B. Grynyov 

National Science Centre, Kharkiv Institute of Physics and Technology, Kharkiv, Ukraine

L. Levchuk 

University of Bristol, Bristol, United Kingdom

D. Anthony , E. Bhal , J.J. Brooke , A. Bundock , E. Clement , D. Cussans , H. Flacher , M. Glowacki, J. Goldstein , H.F. Heath , L. Kreczko , B. Krikler , S. Paramesvaran , S. Seif El Nasr-Storey, V.J. Smith , N. Stylianou⁸² , K. Walkingshaw Pass, R. White

Rutherford Appleton Laboratory, Didcot, United Kingdom

A.H. Ball, K.W. Bell , A. Belyaev⁸³ , C. Brew , R.M. Brown , D.J.A. Cockerill , C. Cooke , K.V. Ellis, K. Harder , S. Harper , M.-L. Holmberg⁸⁴ , Sh. Jain , J. Linacre , K. Manolopoulos, D.M. Newbold , E. Olaiya, D. Petyt , T. Reis , G. Salvi , T. Schuh, C.H. Shepherd-Themistocleous , I.R. Tomalin , T. Williams

Imperial College, London, United Kingdom

R. Bainbridge , P. Bloch , S. Bonomally, J. Borg , C.E. Brown , O. Buchmuller, V. Cacchio, V. Cepaitis , G.S. Chahal⁸⁵ , D. Colling , J.S. Dancu, P. Dauncey , G. Davies , J. Davies, M. Della Negra , S. Fayer, G. Fedi , G. Hall , M.H. Hassanshahi , A. Howard, G. Iles , J. Langford , L. Lyons , A.-M. Magnan , S. Malik, A. Martelli , M. Mieskolainen , D.G. Monk , J. Nash⁸⁶ , M. Pesaresi, B.C. Radburn-Smith , D.M. Raymond, A. Richards, A. Rose , E. Scott , C. Seez , R. Shukla , A. Tapper , K. Uchida , G.P. Uttley , L.H. Vage, T. Virdee²⁷ , M. Vojinovic , N. Wardle , S.N. Webb , D. Winterbottom

Brunel University, Uxbridge, United Kingdom

K. Coldham, J.E. Cole , A. Khan, P. Kyberd , I.D. Reid 

Baylor University, Waco, Texas, USA

S. Abdullin , A. Brinkerhoff , B. Caraway , J. Dittmann , K. Hatakeyama , A.R. Kanuganti , B. McMaster , M. Saunders , S. Sawant , C. Sutantawibul , J. Wilson 

Catholic University of America, Washington, DC, USAR. Bartek , A. Dominguez , R. Uniyal , A.M. Vargas Hernandez **The University of Alabama, Tuscaloosa, Alabama, USA**S.I. Cooper , D. Di Croce , S.V. Gleyzer , C. Henderson , C.U. Perez , P. Rumerio⁸⁷ , C. West **Boston University, Boston, Massachusetts, USA**A. Akpinar , A. Albert , D. Arcaro , C. Cosby , Z. Demiragli , C. Erice , E. Fontanesi , D. Gastler , S. May , J. Rohlf , K. Salyer , D. Sperka , D. Spitzbart , I. Suarez , A. Tsatsos , S. Yuan **Brown University, Providence, Rhode Island, USA**G. Benelli , B. Burkle , X. Coubez²², D. Cutts , M. Hadley , U. Heintz , J.M. Hogan⁸⁸ , T. Kwon , G. Landsberg , K.T. Lau , D. Li , J. Luo , M. Narain , N. Pervan , S. Sagir⁸⁹ , F. Simpson , E. Usai , W.Y. Wong , X. Yan , D. Yu , W. Zhang **University of California, Davis, Davis, California, USA**J. Bonilla , C. Brainerd , R. Breedon , M. Calderon De La Barca Sanchez , M. Chertok , J. Conway , P.T. Cox , R. Erbacher , G. Haza , F. Jensen , O. Kukral , G. Mocellin , M. Mulhearn , D. Pellett , B. Regnery , Y. Yao , F. Zhang **University of California, Los Angeles, California, USA**M. Bachtis , R. Cousins , A. Datta , D. Hamilton , J. Hauser , M. Ignatenko , M.A. Iqbal , T. Lam , E. Manca , W.A. Nash , S. Regnard , D. Saltzberg , B. Stone , V. Valuev **University of California, Riverside, Riverside, California, USA**R. Clare , J.W. Gary , M. Gordon , G. Karapostoli , O.R. Long , N. Manganello , W. Si , S. Wimpenny **University of California, San Diego, La Jolla, California, USA**J.G. Branson , P. Chang , S. Cittolin , S. Cooperstein , D. Diaz , J. Duarte , R. Gerosa , L. Giannini , J. Guiang , R. Kansal , V. Krutelyov , R. Lee , J. Letts , M. Masciovecchio , F. Mokhtar , M. Pieri , B.V. Sathia Narayanan , V. Sharma , M. Tadel , E. Vourliotis , F. Würthwein , Y. Xiang , A. Yagil **University of California, Santa Barbara - Department of Physics, Santa Barbara, California, USA**N. Amin, C. Campagnari , M. Citron , G. Collura , A. Dorsett , V. Dutta , J. Incandela , M. Kilpatrick , J. Kim , A.J. Li , P. Masterson , H. Mei , M. Oshiro , M. Quinnan , J. Richman , U. Sarica , R. Schmitz , F. Setti , J. Sheplock , P. Siddireddy, D. Stuart , S. Wang **California Institute of Technology, Pasadena, California, USA**A. Bornheim , O. Cerri, I. Dutta , A. Latorre, J.M. Lawhorn , J. Mao , H.B. Newman , T. Q. Nguyen , M. Spiropulu , J.R. Vlimant , C. Wang , S. Xie , R.Y. Zhu **Carnegie Mellon University, Pittsburgh, Pennsylvania, USA**J. Alison , S. An , M.B. Andrews , P. Bryant , T. Ferguson , A. Harilal , C. Liu , T. Mudholkar , S. Murthy , M. Paulini , A. Roberts , A. Sanchez , W. Terrill **University of Colorado Boulder, Boulder, Colorado, USA**J.P. Cumalat , W.T. Ford , A. Hassani , G. Karathanasis , E. MacDonald, F. Marini , A. Perloff , C. Savard , N. Schonbeck , K. Stenson , K.A. Ulmer , S.R. Wagner 

N. Zipper 

Cornell University, Ithaca, New York, USA

J. Alexander , S. Bright-Thonney , X. Chen , D.J. Cranshaw , J. Fan , X. Fan , D. Gadkari , S. Hogan , J. Monroy , J.R. Patterson , D. Quach , J. Reichert , M. Reid , A. Ryd , J. Thom , P. Wittich , R. Zou

Fermi National Accelerator Laboratory, Batavia, Illinois, USA

M. Albrow , M. Alyari , G. Apollinari , A. Apresyan , L.A.T. Bauerick , D. Berry , J. Berryhill , P.C. Bhat , K. Burkett , J.N. Butler , A. Canepa , G.B. Cerati , H.W.K. Cheung , F. Chlebana , K.F. Di Petrillo , J. Dickinson , V.D. Elvira , Y. Feng , J. Freeman , A. Gandrakota , Z. Gecse , L. Gray , D. Green, S. Grünendahl , D. Guerrero , O. Gutsche , R.M. Harris , R. Heller , T.C. Herwig , J. Hirschauer , L. Horyn , B. Jayatilaka , S. Jindariani , M. Johnson , U. Joshi , T. Klijnsma , B. Klima , K.H.M. Kwok , S. Lammel , D. Lincoln , R. Lipton , T. Liu , C. Madrid , K. Maeshima , C. Mantilla , D. Mason , P. McBride , P. Merkel , S. Mrenna , S. Nahn , J. Ngadiuba , D. Noonan , V. Papadimitriou , N. Pastika , K. Pedro , C. Pena⁹⁰ , F. Ravera , A. Reinsvold Hall⁹¹ , L. Ristori , E. Sexton-Kennedy , N. Smith , A. Soha , L. Spiegel , J. Strait , L. Taylor , S. Tkaczyk , N.V. Tran , L. Uplegger , E.W. Vaandering , I. Zoi

University of Florida, Gainesville, Florida, USA

P. Avery , D. Bourilkov , L. Cadamuro , V. Cherepanov , R.D. Field, M. Kim, E. Koenig , J. Konigsberg , A. Korytov , E. Kuznetsova , K.H. Lo, K. Matchev , N. Menendez , G. Mitselmakher , A. Muthirakalayil Madhu , N. Rawal , D. Rosenzweig , S. Rosenzweig , K. Shi , J. Wang , Z. Wu

Florida State University, Tallahassee, Florida, USA

T. Adams , A. Askew , N. Bower , R. Habibullah , V. Hagopian , T. Kolberg , G. Martinez, H. Prosper , O. Viazlo , M. Wulansatiti , R. Yohay , J. Zhang

Florida Institute of Technology, Melbourne, Florida, USA

M.M. Baarmand , S. Butalla , T. Elkafrawy⁵⁵ , M. Hohlmann , R. Kumar Verma , M. Rahmani, F. Yumiceva 

University of Illinois Chicago, Chicago, USA, Chicago, USA

M.R. Adams , H. Becerril Gonzalez , R. Cavanaugh , S. Dittmer , O. Evdokimov , C.E. Gerber , D.J. Hofman , D. S. Lemos , A.H. Merrit , C. Mills , G. Oh , T. Roy , S. Rudrabhatla , M.B. Tonjes , N. Varelas , X. Wang , Z. Ye , J. Yoo

The University of Iowa, Iowa City, Iowa, USA

M. Alhusseini , K. Dilsiz⁹² , L. Emediato , G. Karaman , O.K. Köseyan , J.-P. Merlo, A. Mestvirishvili⁹³ , J. Nachtman , O. Neogi, H. Ogul⁹⁴ , Y. Onel , A. Penzo , C. Snyder, E. Tiras⁹⁵

Johns Hopkins University, Baltimore, Maryland, USA

O. Amram , B. Blumenfeld , L. Corcodilos , J. Davis , A.V. Gritsan , S. Kyriacou , P. Maksimovic , J. Roskes , S. Sekhar , M. Swartz , T.Á. Vámi

The University of Kansas, Lawrence, Kansas, USA

A. Abreu , L.F. Alcerro Alcerro , J. Anguiano , P. Baringer , A. Bean , Z. Flowers , T. Isidori , J. King , G. Krintiras , M. Lazarovits , C. Le Mahieu , C. Lindsey, J. Marquez , N. Minafra , M. Murray , M. Nickel , C. Rogan , C. Royon , R. Salvatico , S. Sanders , C. Smith , Q. Wang , G. Wilson

Kansas State University, Manhattan, Kansas, USA

B. Allmond , S. Duric, A. Ivanov , K. Kaadze , A. Kalogeropoulos , D. Kim, Y. Maravin , T. Mitchell, A. Modak, K. Nam, D. Roy 

Lawrence Livermore National Laboratory, Livermore, California, USA

F. Rebassoo , D. Wright 

University of Maryland, College Park, Maryland, USA

E. Adams , A. Baden , O. Baron, A. Belloni , A. Bethani , S.C. Eno , N.J. Hadley , S. Jabeen , R.G. Kellogg , T. Koeth , Y. Lai , S. Lascio , A.C. Mignerey , S. Nabili , C. Palmer , C. Papageorgakis , L. Wang , K. Wong 

Massachusetts Institute of Technology, Cambridge, Massachusetts, USA

D. Abercrombie, W. Busza , I.A. Cali , Y. Chen , M. D'Alfonso , J. Eysermans , C. Freer , G. Gomez-Ceballos , M. Goncharov, P. Harris, M. Hu , D. Kovalskyi , J. Krupa , Y.-J. Lee , K. Long , C. Mironov , C. Paus , D. Rankin , C. Roland , G. Roland , Z. Shi , G.S.F. Stephans , J. Wang, Z. Wang , B. Wyslouch , T. J. Yang 

University of Minnesota, Minneapolis, Minnesota, USA

R.M. Chatterjee, B. Crossman , A. Evans , J. Hiltbrand , B.M. Joshi , C. Kapsiak , M. Krohn , Y. Kubota , J. Mans , M. Revering , R. Rusack , R. Saradhy , N. Schroeder , N. Strobbe , M.A. Wadud 

University of Mississippi, Oxford, Mississippi, USA

L.M. Cremaldi 

University of Nebraska-Lincoln, Lincoln, Nebraska, USA

K. Bloom , M. Bryson, D.R. Claes , C. Fangmeier , L. Finco , F. Golf , C. Joo , R. Kamaliuddin, I. Kravchenko , I. Reed , J.E. Siado , G.R. Snow[†], W. Tabb , A. Wightman , F. Yan , A.G. Zecchinelli 

State University of New York at Buffalo, Buffalo, New York, USA

G. Agarwal , H. Bandyopadhyay , L. Hay , I. Iashvili , A. Kharchilava , C. McLean , M. Morris , D. Nguyen , J. Pekkanen , S. Rappoccio , A. Williams 

Northeastern University, Boston, Massachusetts, USA

G. Alverson , E. Barberis , Y. Haddad , Y. Han , A. Krishna , J. Li , J. Lidrych , G. Madigan , B. Marzocchi , D.M. Morse , V. Nguyen , T. Orimoto , A. Parker , L. Skinnari , A. Tishelman-Charny , T. Wamorkar , B. Wang , A. Wisecarver , D. Wood 

Northwestern University, Evanston, Illinois, USA

S. Bhattacharya , J. Bueghly, Z. Chen , A. Gilbert , K.A. Hahn , Y. Liu , N. Odell , M.H. Schmitt , M. Velasco

University of Notre Dame, Notre Dame, Indiana, USA

R. Band , R. Bucci, M. Cremonesi, A. Das , R. Goldouzian , M. Hildreth , K. Hurtado Anampa , C. Jessop , K. Lannon , J. Lawrence , N. Loukas , L. Lutton , J. Mariano, N. Marinelli, I. Mcalister, T. McCauley , C. Mcgrady , K. Mohrman , C. Moore , Y. Musienko¹² , R. Ruchti , A. Townsend , M. Wayne , H. Yockey, M. Zarucki , L. Zygal 

The Ohio State University, Columbus, Ohio, USA

B. Bylsma, M. Carrigan , L.S. Durkin , B. Francis , C. Hill , M. Joyce , A. Lesauvage , M. Nunez Ornelas , K. Wei, B.L. Winer , B. R. Yates 

Princeton University, Princeton, New Jersey, USA

F.M. Addesa [ID](#), P. Das [ID](#), G. Dezoort [ID](#), P. Elmer [ID](#), A. Frankenthal [ID](#), B. Greenberg [ID](#), N. Haubrich [ID](#), S. Higginbotham [ID](#), G. Kopp [ID](#), S. Kwan [ID](#), D. Lange [ID](#), D. Marlow [ID](#), I. Ojalvo [ID](#), J. Olsen [ID](#), D. Stickland [ID](#), C. Tully [ID](#)

University of Puerto Rico, Mayaguez, Puerto Rico, USA

S. Malik [ID](#), S. Norberg

Purdue University, West Lafayette, Indiana, USA

A.S. Bakshi [ID](#), V.E. Barnes [ID](#), R. Chawla [ID](#), S. Das [ID](#), L. Gutay, M. Jones [ID](#), A.W. Jung [ID](#), D. Kondratyev [ID](#), A.M. Koshy, M. Liu [ID](#), G. Negro [ID](#), N. Neumeister [ID](#), G. Paspalaki [ID](#), S. Piperov [ID](#), A. Purohit [ID](#), J.F. Schulte [ID](#), M. Stojanovic [ID](#), J. Thieman [ID](#), F. Wang [ID](#), R. Xiao [ID](#), W. Xie [ID](#)

Purdue University Northwest, Hammond, Indiana, USA

J. Dolen [ID](#), N. Parashar [ID](#)

Rice University, Houston, Texas, USA

D. Acosta [ID](#), A. Baty [ID](#), T. Carnahan [ID](#), S. Dildick [ID](#), K.M. Ecklund [ID](#), P.J. Fernández Manteca [ID](#), S. Freed, P. Gardner, F.J.M. Geurts [ID](#), A. Kumar [ID](#), W. Li [ID](#), B.P. Padley [ID](#), R. Redjimi, J. Rotter [ID](#), S. Yang [ID](#), E. Yigitbasi [ID](#), L. Zhang⁹⁶, Y. Zhang [ID](#)

University of Rochester, Rochester, New York, USA

A. Bodek [ID](#), P. de Barbaro [ID](#), R. Demina [ID](#), J.L. Dulemba [ID](#), C. Fallon, T. Ferbel [ID](#), M. Galanti, A. Garcia-Bellido [ID](#), O. Hindrichs [ID](#), A. Khukhunaishvili [ID](#), P. Parygin [ID](#), E. Popova [ID](#), E. Ranken [ID](#), R. Taus [ID](#), G.P. Van Onsem [ID](#)

The Rockefeller University, New York, New York, USA

K. Goulianatos [ID](#)

Rutgers, The State University of New Jersey, Piscataway, New Jersey, USA

B. Chiarito, J.P. Chou [ID](#), Y. Gershtain [ID](#), E. Halkiadakis [ID](#), A. Hart [ID](#), M. Heindl [ID](#), D. Jaroslawski [ID](#), O. Karacheban²⁵ [ID](#), I. Laflotte [ID](#), A. Lath [ID](#), R. Montalvo, K. Nash, M. Osherson [ID](#), H. Routray [ID](#), S. Salur [ID](#), S. Schnetzer, S. Somalwar [ID](#), R. Stone [ID](#), S.A. Thayil [ID](#), S. Thomas, H. Wang [ID](#)

University of Tennessee, Knoxville, Tennessee, USA

H. Acharya, A.G. Delannoy [ID](#), S. Fiorendi [ID](#), T. Holmes [ID](#), E. Nibigira [ID](#), S. Spanier [ID](#)

Texas A&M University, College Station, Texas, USA

O. Bouhali⁹⁷ [ID](#), M. Dalchenko [ID](#), A. Delgado [ID](#), R. Eusebi [ID](#), J. Gilmore [ID](#), T. Huang [ID](#), T. Kamon⁹⁸ [ID](#), H. Kim [ID](#), S. Luo [ID](#), S. Malhotra, R. Mueller [ID](#), D. Overton [ID](#), D. Rathjens [ID](#), A. Safonov [ID](#)

Texas Tech University, Lubbock, Texas, USA

N. Akchurin [ID](#), J. Damgov [ID](#), V. Hegde [ID](#), K. Lamichhane [ID](#), S.W. Lee [ID](#), T. Mengke, S. Muthumuni [ID](#), T. Peltola [ID](#), I. Volobouev [ID](#), A. Whitbeck [ID](#)

Vanderbilt University, Nashville, Tennessee, USA

E. Appelt [ID](#), S. Greene, A. Gurrola [ID](#), W. Johns [ID](#), A. Melo [ID](#), F. Romeo [ID](#), P. Sheldon [ID](#), S. Tuo [ID](#), J. Velkovska [ID](#), J. Viinikainen [ID](#)

University of Virginia, Charlottesville, Virginia, USA

B. Cardwell [ID](#), B. Cox [ID](#), G. Cummings [ID](#), J. Hakala [ID](#), R. Hirosky [ID](#), A. Ledovskoy [ID](#), A. Li [ID](#), C. Neu [ID](#), C.E. Perez Lara [ID](#), B. Tannenwald [ID](#)

Wayne State University, Detroit, Michigan, USAP.E. Karchin , N. Poudyal **University of Wisconsin - Madison, Madison, Wisconsin, USA**S. Banerjee , K. Black , T. Bose , S. Dasu , I. De Bruyn , P. Everaerts , C. Galloni, H. He , M. Herndon , A. Herve , C.K. Koraka , A. Lanaro, A. Loeliger , R. Loveless , J. Madhusudanan Sreekala , A. Mallampalli , A. Mohammadi , S. Mondal, G. Parida , D. Pinna, A. Savin, V. Shang , V. Sharma , W.H. Smith , D. Teague, H.F. Tsoi , W. Vetens **Authors affiliated with an institute or an international laboratory covered by a cooperation agreement with CERN**S. Afanasiev , V. Andreev , Yu. Andreev , T. Aushev , M. Azarkin , A. Babaev , A. Belyaev , V. Blinov⁹⁹, E. Boos , V. Borshch , D. Budkouski , V. Bunichev , V. Chekhovsky, R. Chistov⁹⁹ , M. Danilov⁹⁹ , A. Dermenev , T. Dimova⁹⁹ , I. Dremin , M. Dubinin⁹⁰ , L. Dudko , V. Epshteyn , G. Gavrilov , V. Gavrilov , S. Gnenenko , V. Golovtcov , N. Golubev , I. Golutvin , I. Gorbunov , A. Gribushin , Y. Ivanov , V. Kachanov , L. Kardapoltsev⁹⁹ , V. Karjavine , A. Karneyeu , V. Kim⁹⁹ , M. Kirakosyan, D. Kirpichnikov , M. Kirsanov , V. Klyukhin , D. Konstantinov , V. Korenkov , A. Kozyrev⁹⁹ , N. Krasnikov , A. Lanev , P. Levchenko , A. Litomin, N. Lychkovskaya , V. Makarenko , A. Malakhov , V. Matveev⁹⁹ , V. Murzin , A. Nikitenko¹⁰⁰ , S. Obraztsov , A. Oskin, I. Ovtin⁹⁹ , V. Palichik , V. Perelygin , M. Perfilov, S. Petrushanko , S. Polikarpov⁹⁹ , V. Popov, O. Radchenko⁹⁹ , M. Savina , V. Savrin , V. Shalaev , S. Shmatov , S. Shulha , Y. Skovpen⁹⁹ , S. Slabospitskii , V. Smirnov , D. Sosnov , V. Sulimov , E. Tcherniaev , A. Terkulov , O. Teryaev , I. Tlisova , M. Toms , A. Toropin , L. Uvarov , A. Uzunian , E. Vlasov , P. Volkov , A. Vorobyev, N. Voytishin , B.S. Yuldashev¹⁰¹, A. Zarubin , I. Zhizhin , A. Zhokin

†: Deceased

¹Also at Yerevan State University, Yerevan, Armenia²Also at TU Wien, Vienna, Austria³Also at Institute of Basic and Applied Sciences, Faculty of Engineering, Arab Academy for Science, Technology and Maritime Transport, Alexandria, Egypt⁴Also at Université Libre de Bruxelles, Bruxelles, Belgium⁵Also at Universidade Estadual de Campinas, Campinas, Brazil⁶Also at Federal University of Rio Grande do Sul, Porto Alegre, Brazil⁷Also at UFMS, Nova Andradina, Brazil⁸Also at University of Chinese Academy of Sciences, Beijing, China⁹Also at Nanjing Normal University, Nanjing, China¹⁰Now at The University of Iowa, Iowa City, Iowa, USA¹¹Also at University of Chinese Academy of Sciences, Beijing, China¹²Also at an institute or an international laboratory covered by a cooperation agreement with CERN¹³Also at Cairo University, Cairo, Egypt¹⁴Also at Suez University, Suez, Egypt¹⁵Now at British University in Egypt, Cairo, Egypt¹⁶Also at Purdue University, West Lafayette, Indiana, USA¹⁷Also at Université de Haute Alsace, Mulhouse, France¹⁸Also at Department of Physics, Tsinghua University, Beijing, China¹⁹Also at The University of the State of Amazonas, Manaus, Brazil²⁰Also at Erzincan Binali Yildirim University, Erzincan, Turkey

- ²¹Also at University of Hamburg, Hamburg, Germany
- ²²Also at RWTH Aachen University, III. Physikalisches Institut A, Aachen, Germany
- ²³Also at Isfahan University of Technology, Isfahan, Iran
- ²⁴Also at Bergische University Wuppertal (BUW), Wuppertal, Germany
- ²⁵Also at Brandenburg University of Technology, Cottbus, Germany
- ²⁶Also at Forschungszentrum Jülich, Juelich, Germany
- ²⁷Also at CERN, European Organization for Nuclear Research, Geneva, Switzerland
- ²⁸Also at Physics Department, Faculty of Science, Assiut University, Assiut, Egypt
- ²⁹Also at Karoly Robert Campus, MATE Institute of Technology, Gyongyos, Hungary
- ³⁰Also at Wigner Research Centre for Physics, Budapest, Hungary
- ³¹Also at Institute of Physics, University of Debrecen, Debrecen, Hungary
- ³²Also at Institute of Nuclear Research ATOMKI, Debrecen, Hungary
- ³³Now at Universitatea Babes-Bolyai - Facultatea de Fizica, Cluj-Napoca, Romania
- ³⁴Also at Faculty of Informatics, University of Debrecen, Debrecen, Hungary
- ³⁵Also at Punjab Agricultural University, Ludhiana, India
- ³⁶Also at UPES - University of Petroleum and Energy Studies, Dehradun, India
- ³⁷Also at University of Visva-Bharati, Santiniketan, India
- ³⁸Also at University of Hyderabad, Hyderabad, India
- ³⁹Also at Indian Institute of Science (IISc), Bangalore, India
- ⁴⁰Also at Indian Institute of Technology (IIT), Mumbai, India
- ⁴¹Also at IIT Bhubaneswar, Bhubaneswar, India
- ⁴²Also at Institute of Physics, Bhubaneswar, India
- ⁴³Also at Deutsches Elektronen-Synchrotron, Hamburg, Germany
- ⁴⁴Now at Department of Physics, Isfahan University of Technology, Isfahan, Iran
- ⁴⁵Also at Sharif University of Technology, Tehran, Iran
- ⁴⁶Also at Department of Physics, University of Science and Technology of Mazandaran, Behshahr, Iran
- ⁴⁷Also at Helwan University, Cairo, Egypt
- ⁴⁸Also at Italian National Agency for New Technologies, Energy and Sustainable Economic Development, Bologna, Italy
- ⁴⁹Also at Centro Siciliano di Fisica Nucleare e di Struttura Della Materia, Catania, Italy
- ⁵⁰Also at Università degli Studi Guglielmo Marconi, Roma, Italy
- ⁵¹Also at Scuola Superiore Meridionale, Università di Napoli 'Federico II', Napoli, Italy
- ⁵²Also at Fermi National Accelerator Laboratory, Batavia, Illinois, USA
- ⁵³Also at Laboratori Nazionali di Legnaro dell'INFN, Legnaro, Italy
- ⁵⁴Also at Università di Napoli 'Federico II', Napoli, Italy
- ⁵⁵Also at Ain Shams University, Cairo, Egypt
- ⁵⁶Also at Consiglio Nazionale delle Ricerche - Istituto Officina dei Materiali, Perugia, Italy
- ⁵⁷Also at Department of Applied Physics, Faculty of Science and Technology, Universiti Kebangsaan Malaysia, Bangi, Malaysia
- ⁵⁸Also at Consejo Nacional de Ciencia y Tecnología, Mexico City, Mexico
- ⁵⁹Also at IRFU, CEA, Université Paris-Saclay, Gif-sur-Yvette, France
- ⁶⁰Also at Faculty of Physics, University of Belgrade, Belgrade, Serbia
- ⁶¹Also at Trincomalee Campus, Eastern University, Sri Lanka, Nilaveli, Sri Lanka
- ⁶²Also at Saegis Campus, Nugegoda, Sri Lanka
- ⁶³Also at INFN Sezione di Pavia, Università di Pavia, Pavia, Italy
- ⁶⁴Also at National and Kapodistrian University of Athens, Athens, Greece
- ⁶⁵Also at Ecole Polytechnique Fédérale Lausanne, Lausanne, Switzerland
- ⁶⁶Also at Universität Zürich, Zurich, Switzerland

⁶⁷Also at Stefan Meyer Institute for Subatomic Physics, Vienna, Austria

⁶⁸Also at Laboratoire d'Annecy-le-Vieux de Physique des Particules, IN2P3-CNRS, Annecy-le-Vieux, France

⁶⁹Also at Near East University, Research Center of Experimental Health Science, Mersin, Turkey

⁷⁰Also at Konya Technical University, Konya, Turkey

⁷¹Also at Izmir Bakircay University, Izmir, Turkey

⁷²Also at Adiyaman University, Adiyaman, Turkey

⁷³Also at Istanbul Gedik University, Istanbul, Turkey

⁷⁴Also at Necmettin Erbakan University, Konya, Turkey

⁷⁵Also at Bozok Universitetesi Rektörlüğü, Yozgat, Turkey

⁷⁶Also at Marmara University, Istanbul, Turkey

⁷⁷Also at Milli Savunma University, Istanbul, Turkey

⁷⁸Also at Kafkas University, Kars, Turkey

⁷⁹Also at Hacettepe University, Ankara, Turkey

⁸⁰Also at Istanbul University - Cerrahpasa, Faculty of Engineering, Istanbul, Turkey

⁸¹Also at Ozyegin University, Istanbul, Turkey

⁸²Also at Vrije Universiteit Brussel, Brussel, Belgium

⁸³Also at School of Physics and Astronomy, University of Southampton, Southampton, United Kingdom

⁸⁴Also at University of Bristol, Bristol, United Kingdom

⁸⁵Also at IPPP Durham University, Durham, United Kingdom

⁸⁶Also at Monash University, Faculty of Science, Clayton, Australia

⁸⁷Also at Università di Torino, Torino, Italy

⁸⁸Also at Bethel University, St. Paul, Minnesota, USA

⁸⁹Also at Karamanoğlu Mehmetbey University, Karaman, Turkey

⁹⁰Also at California Institute of Technology, Pasadena, California, USA

⁹¹Also at United States Naval Academy, Annapolis, Maryland, USA

⁹²Also at Bingöl University, Bingöl, Turkey

⁹³Also at Georgian Technical University, Tbilisi, Georgia

⁹⁴Also at Sinop University, Sinop, Turkey

⁹⁵Also at Erciyes University, Kayseri, Turkey

⁹⁶Also at Institute of Modern Physics and Key Laboratory of Nuclear Physics and Ion-beam Application (MOE) - Fudan University, Shanghai, China

⁹⁷Also at Texas A&M University at Qatar, Doha, Qatar

⁹⁸Also at Kyungpook National University, Daegu, Korea

⁹⁹Also at another institute or international laboratory covered by a cooperation agreement with CERN

¹⁰⁰Also at Imperial College, London, United Kingdom

¹⁰¹Also at Institute of Nuclear Physics of the Uzbekistan Academy of Sciences, Tashkent, Uzbekistan